PUNCIÓN TRANSBRONQUIAL

E. García-Ureta
La Coruña
España

2011
ZARAGOZA

SEAP-IAP

sec

SEPAR

Schieppati E.

La punción mediastinal a través del espolón traqueal.
Rev As Med Argent 1949; 663:497-499.

Wang KP.

Am Rev Resoir Dis 1978; 118: 17-21.

Wang KP.

Chest 1981; 80: 48-50.

Wang KP.

Am Rev Respir Dis 1983; 127: 344-347.

Wang KP.

Ann Otol Rhinol Laryngol 1985; 94: 382-385.

INDICACIONES

Estadiaje del cáncer de pulmón

Diagnóstico de tumores intrapulmonares

Diagnóstico de adenopatías hiliares y mediastínicas

Diagnóstico de tumores mediastínicos

MUESTRA ADECUADA

Bien Preservada

Material Suficiente

Técnicas Especiales

ASPECTOS

Clínicos

Radiológicos

Citológicos

ESPECIFICIDAD

FALSOS POSITIVOS

100%

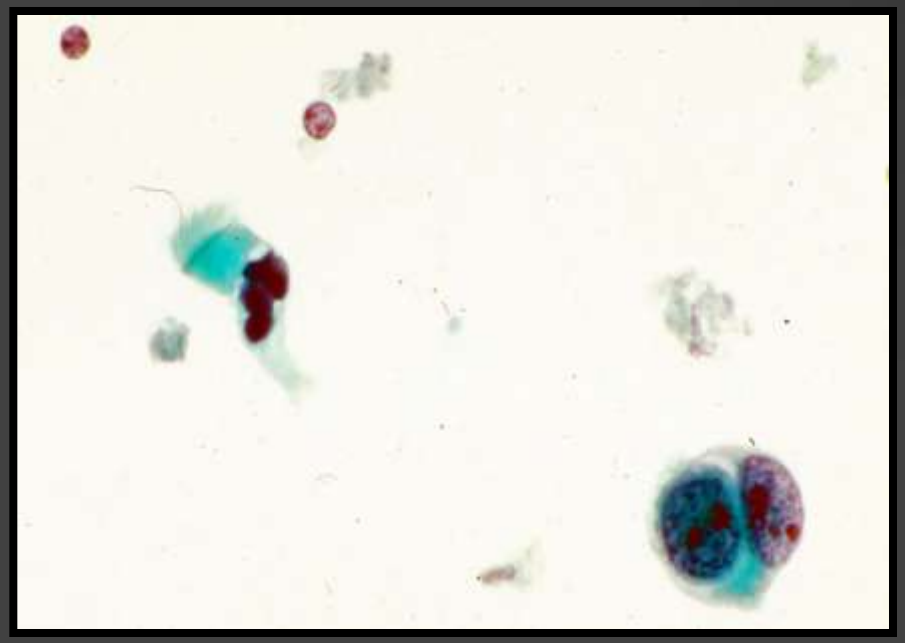

Cropp AJ.

Chest 1984; 85: 696-697.

Carlin BW.

Am Rev Respir Dis 1989; 140: 1800-1802.

SENSIBILIDAD

Shure D.

Chest 1984; 86: 693-696. 15%

Schenk DA.

Am Rev Respir Dis 1986; 134: 146-148. >85%

SENSIBILIDAD

Tamaño
Localización
Tipo de aguja
Nº de aspirados
Valoración in situ
Naturaleza de la lesión

Experiencia del Broncoscopista

FORMACIÓN

- **3 AÑOS** 21.4 al 47.6 %
- 10.5 – 2 % Insatisfactorios
- HAPONIK

Care Med 1998;151:1998-2002

- **2 AÑOS** 32 al 78 %
- 50 Técnicas.
- CASTRO

Chest. 1997;111:103-105

- 25 Técnicas 10 por año
- ERNST

Chest 2003;123:1693-1717.

COMPLICACIONES

- Neumotorax
- Neumomediastino
- Hemomediastino
- Bacteriemia
- Pericarditis

Shin H.J.

Cancer 2002; 96: 174-180

0% - 2%

INCONVENIENTES

Dificultad Técnica

Localización Tumor

Peligrosidad-Grandes Vasos

Manipulación

Falsos Negativos

Muestras Pequeñas

Secado

Bloque Celular

CARCINOIDE

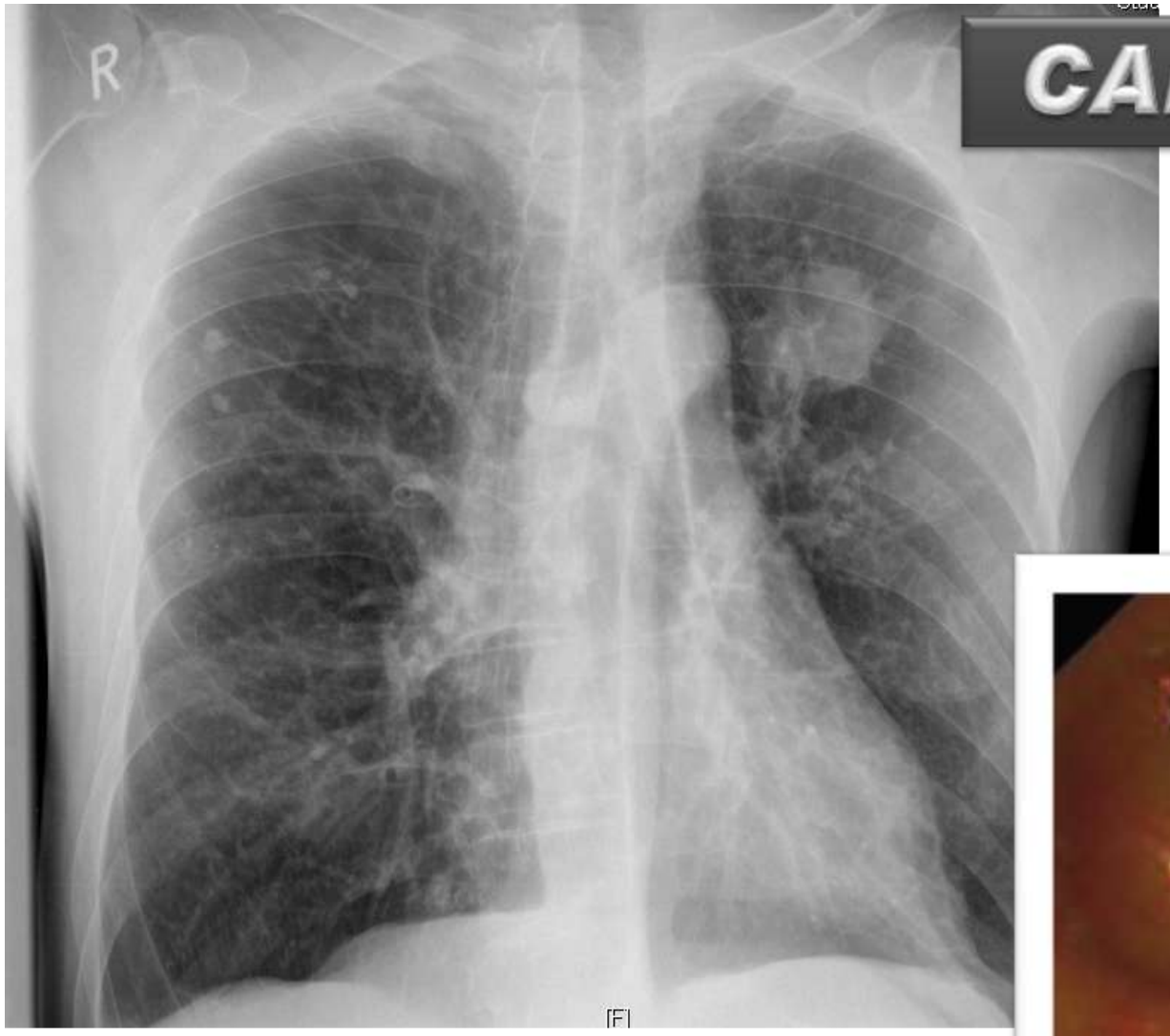

Varón de 63 años.
Fumador importante.
RX. tórax : lesión en LSI.

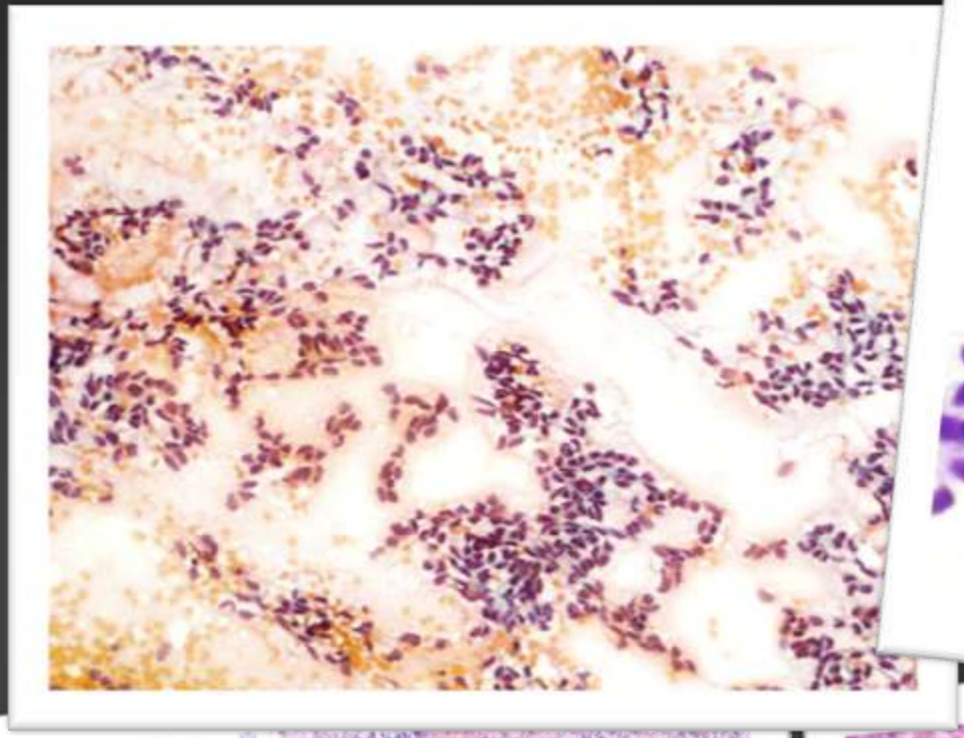

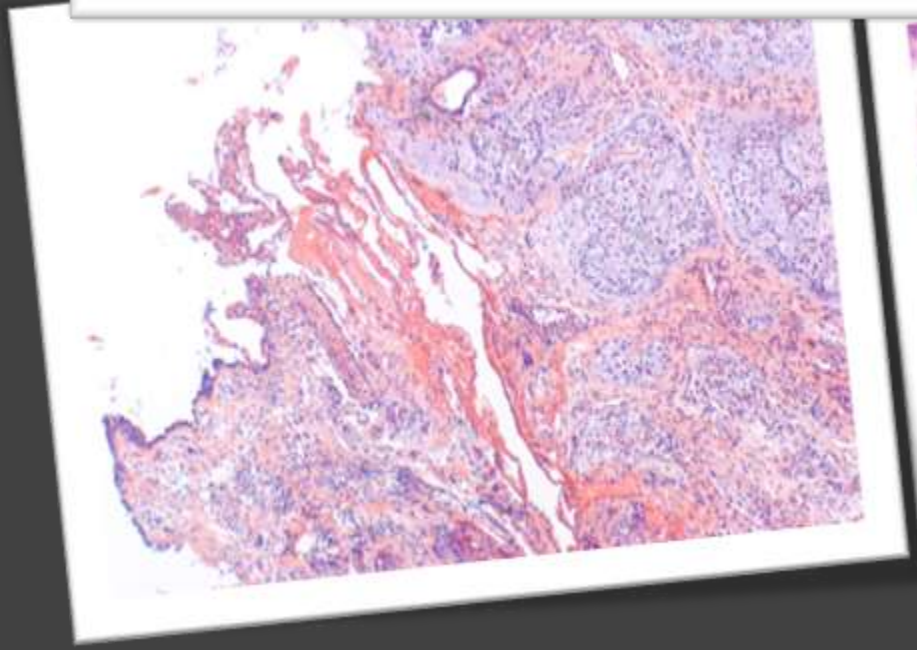

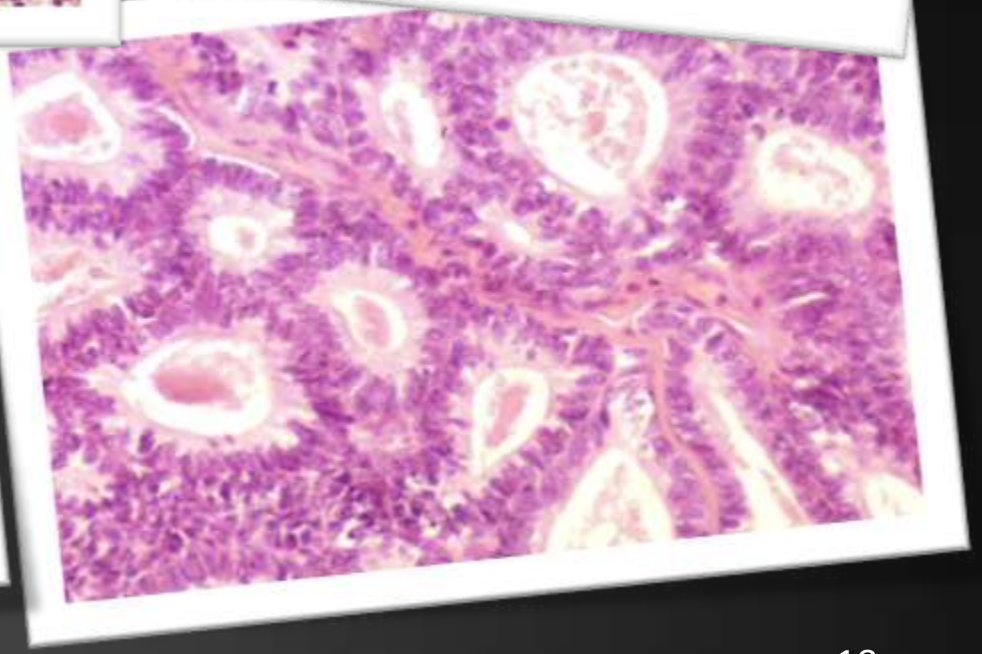

LESIONES EXOFÍTICAS

- Necrosis .
- Muestra Inadecuada.
- Artefacto de Aplastamiento.

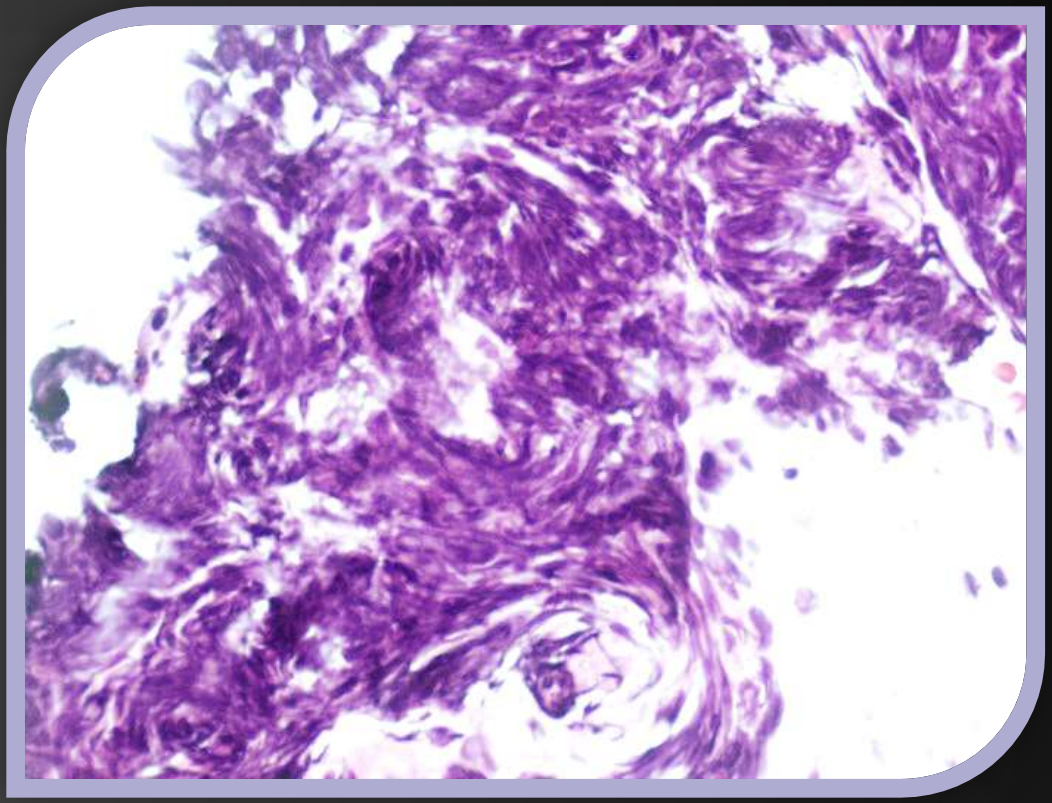

CARCINOMA de C. GRANDES

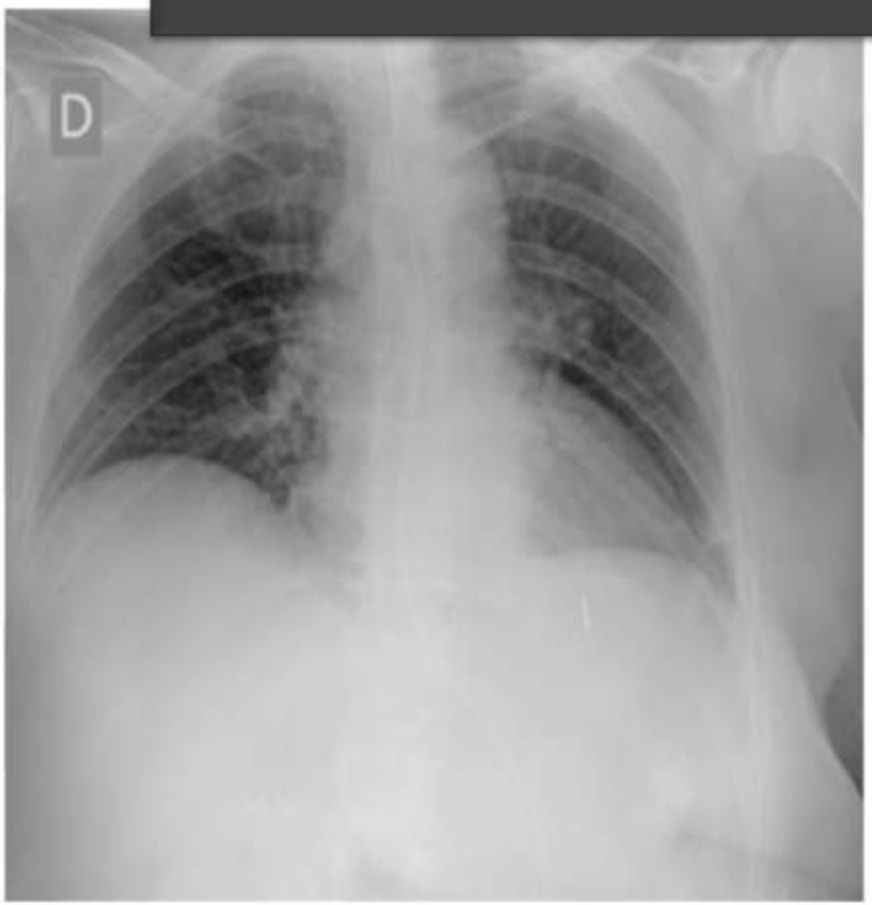

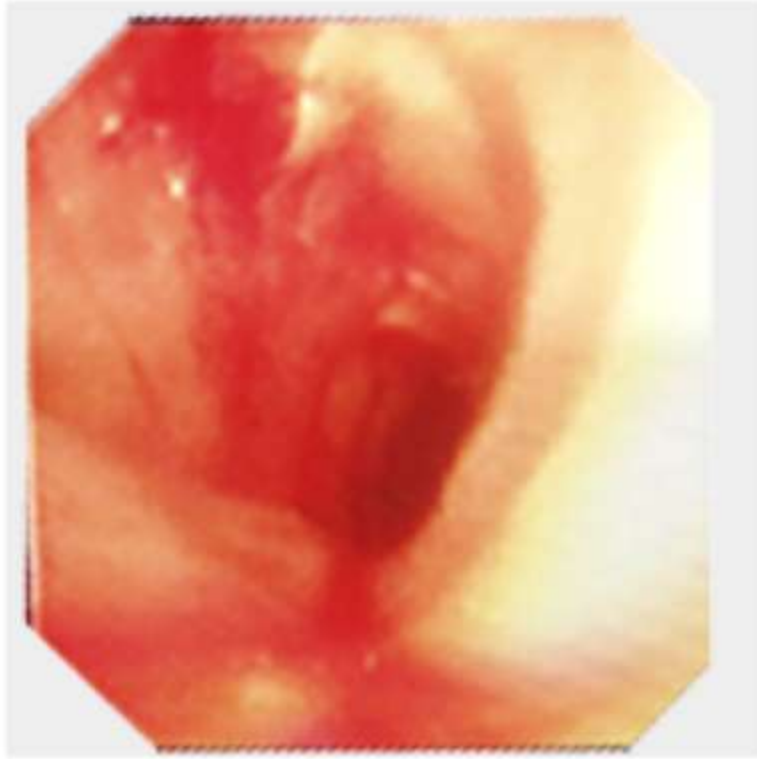

Mujer 65 años
Masa en LSI
Infiltración Submucosa

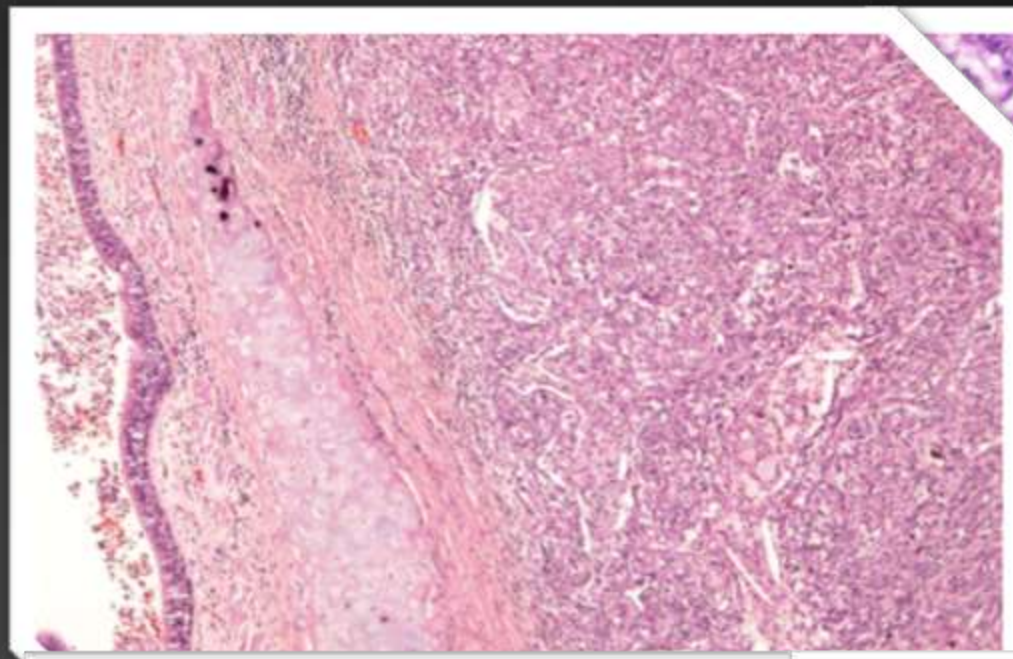
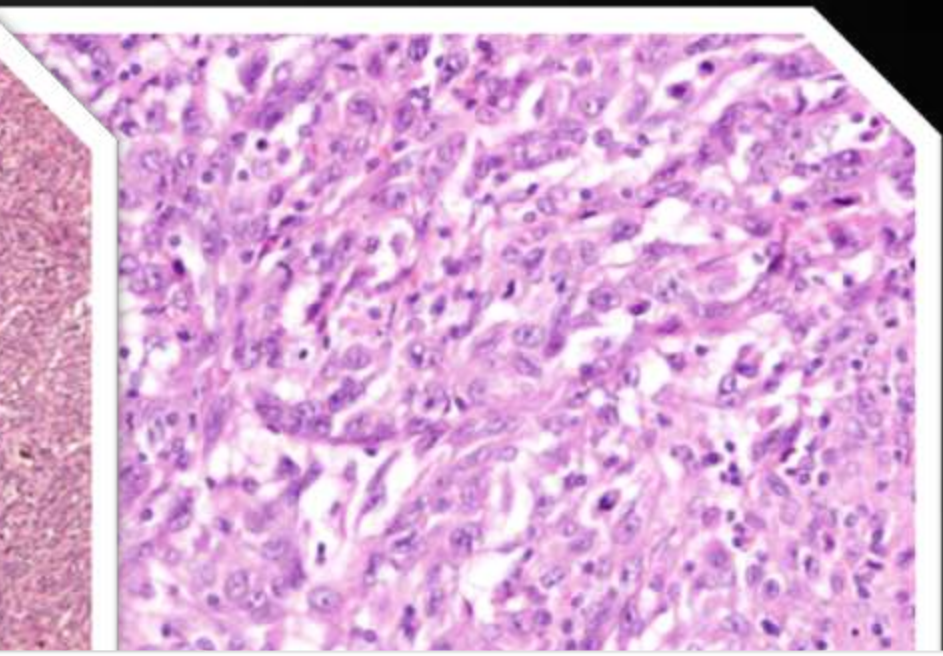
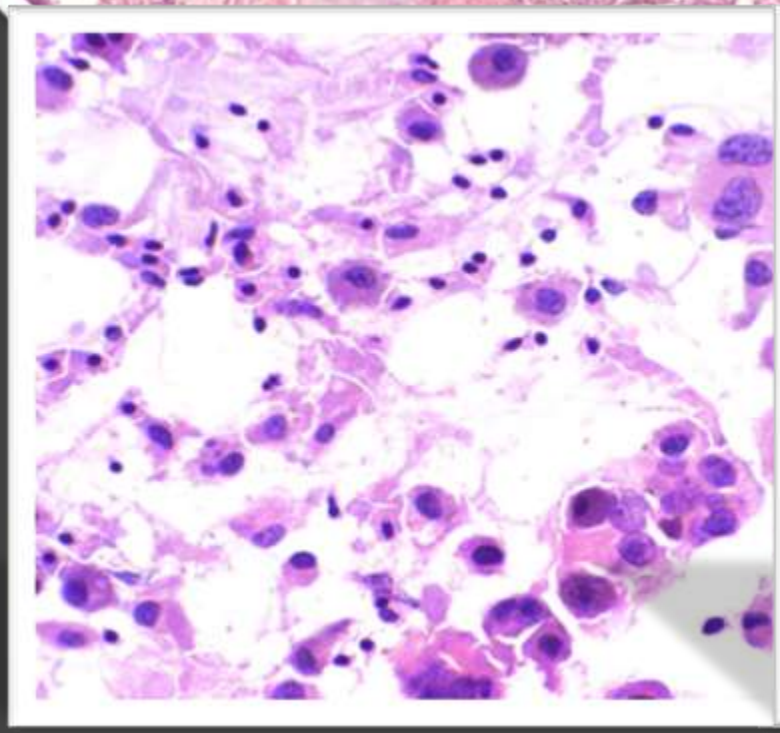
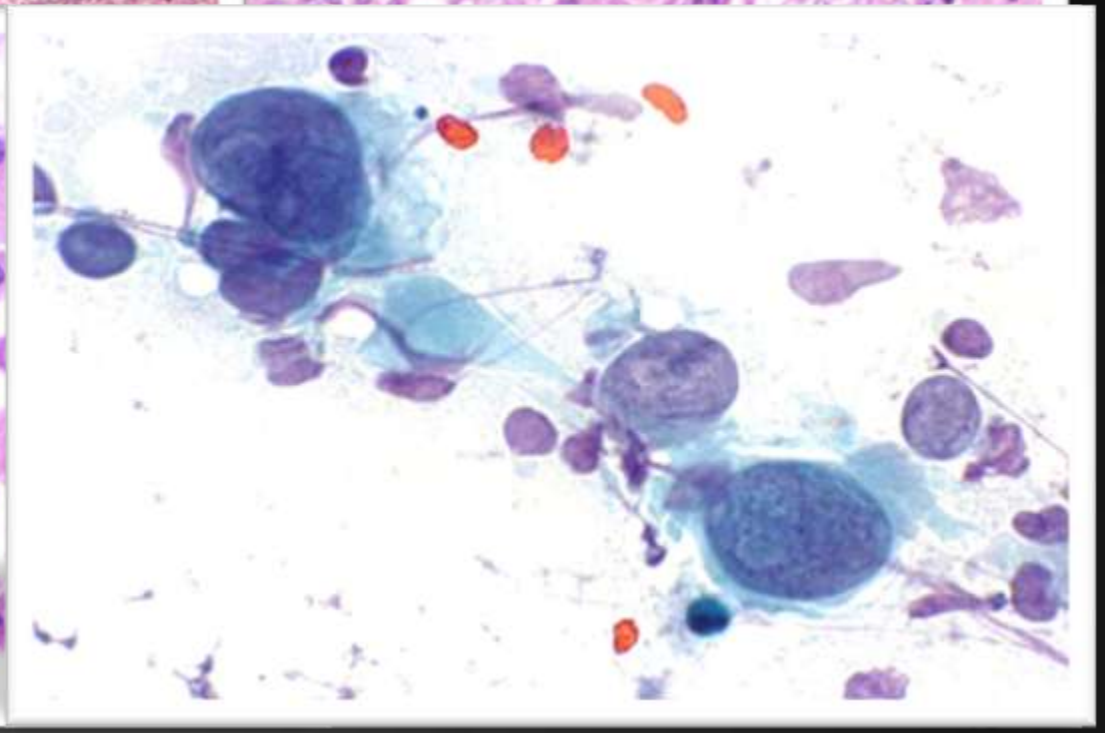

MASAS MEDIASTÍNICAS

Tumores Primarios

Metástasis Ganglionares

Enfermedad no Neoplásica

SARCOIDOSIS

Kelly SJ.

J Thorac Imaging 1987; 2: 33-40.

Morales MCF.

Chest 1994; 106: 709-711.

Bilaceroglu S

Monaldi Arch Chest Dis 1999; 54: 217-213.

Trisolini R.

Chest 2003; 124: 2126-2130.

Bilaceroglu S

J Bronchol 2004; 11: 54-61.

Annema JT

Eur Respir J 2005; 25: 405-9

TBC

Baran R.

Thorax 1996; 51: 87-89.

Cetinkaya E.

Respiration 2002; 69: 335-338.

Bilaçeroglu S.

Chest 2004; 126: 259-267.

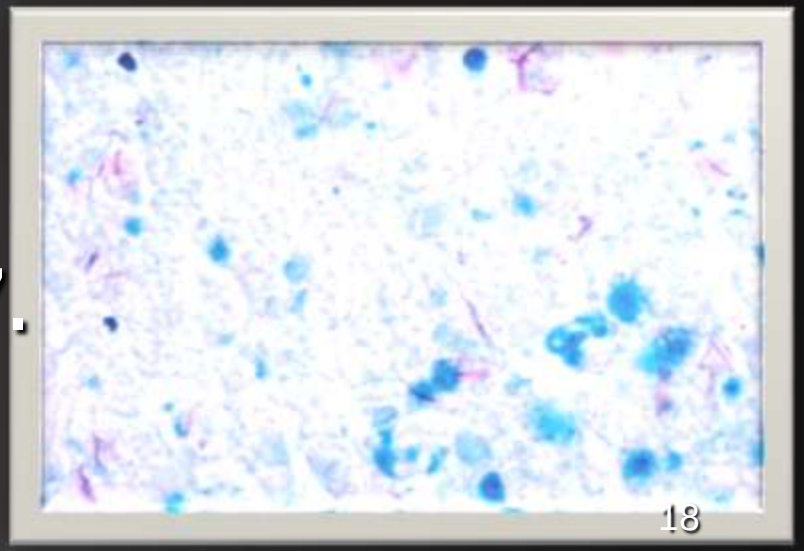

MELANOMA

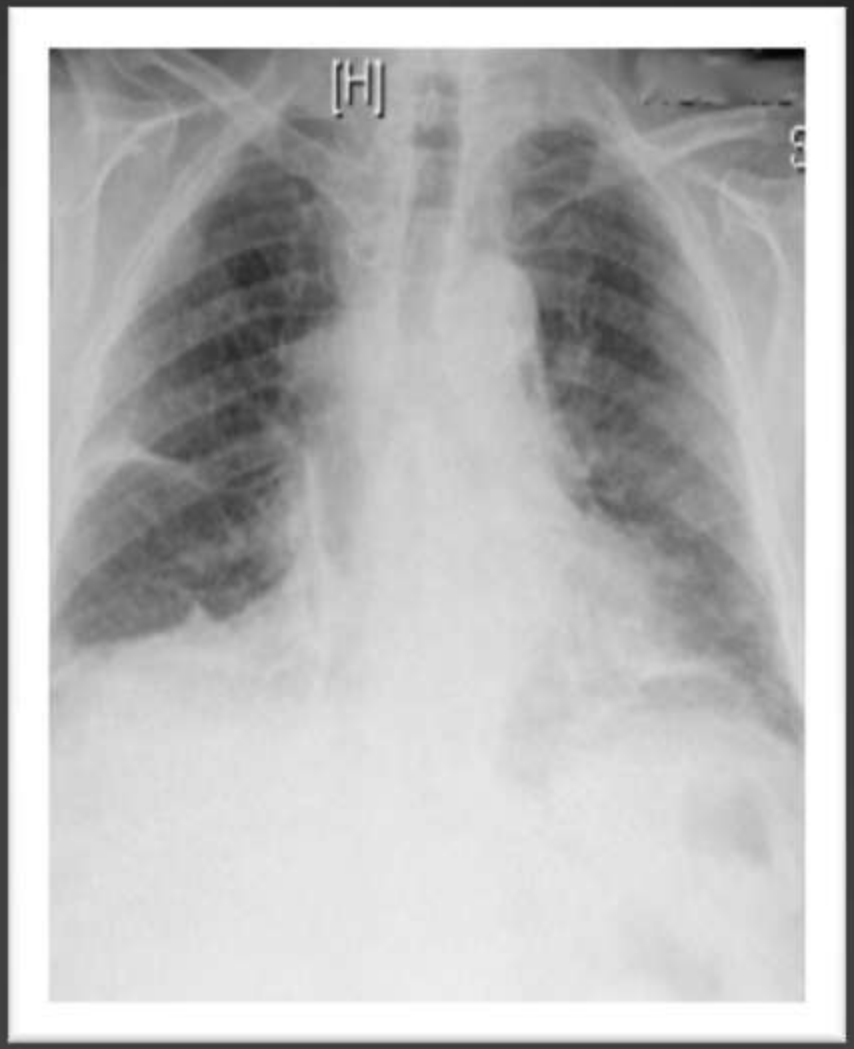

Varón 56 años

Masa Pulmonar

Adenopatias Mediastinicas

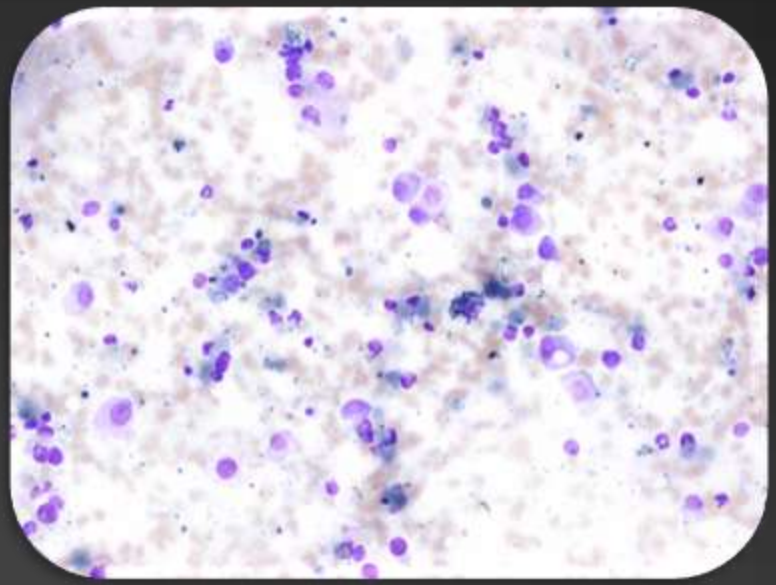

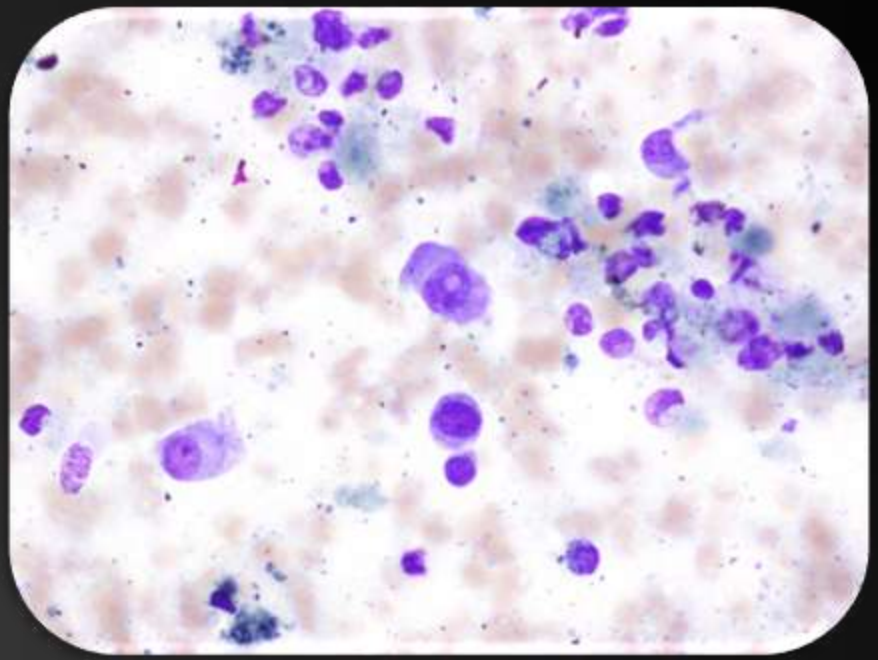

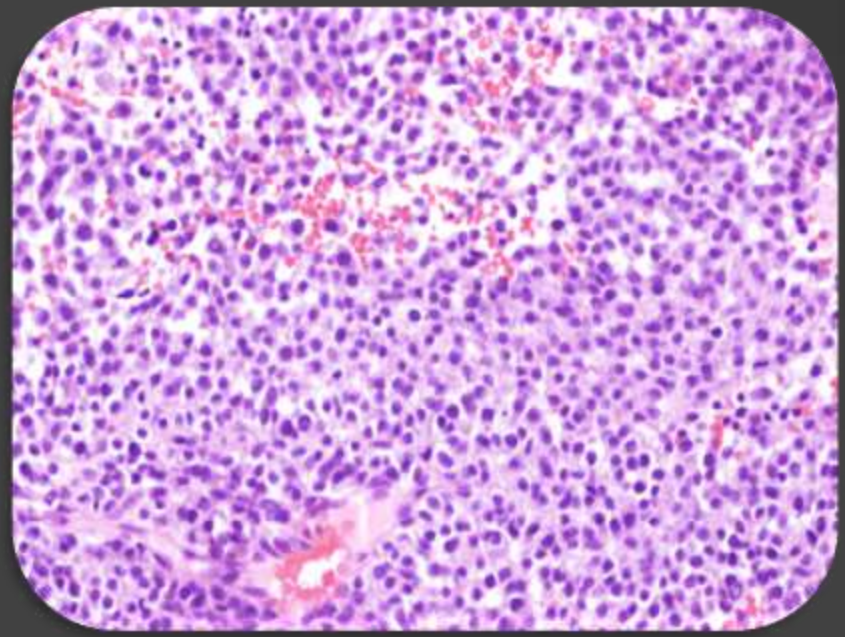

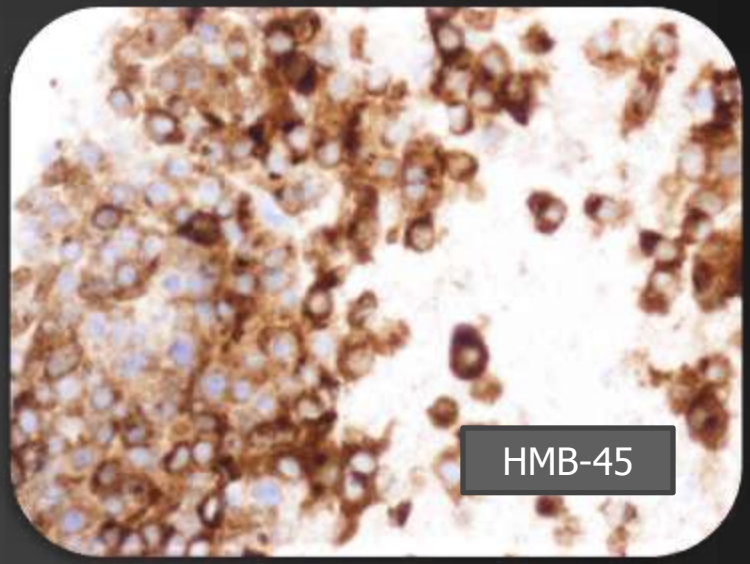
HMB-45

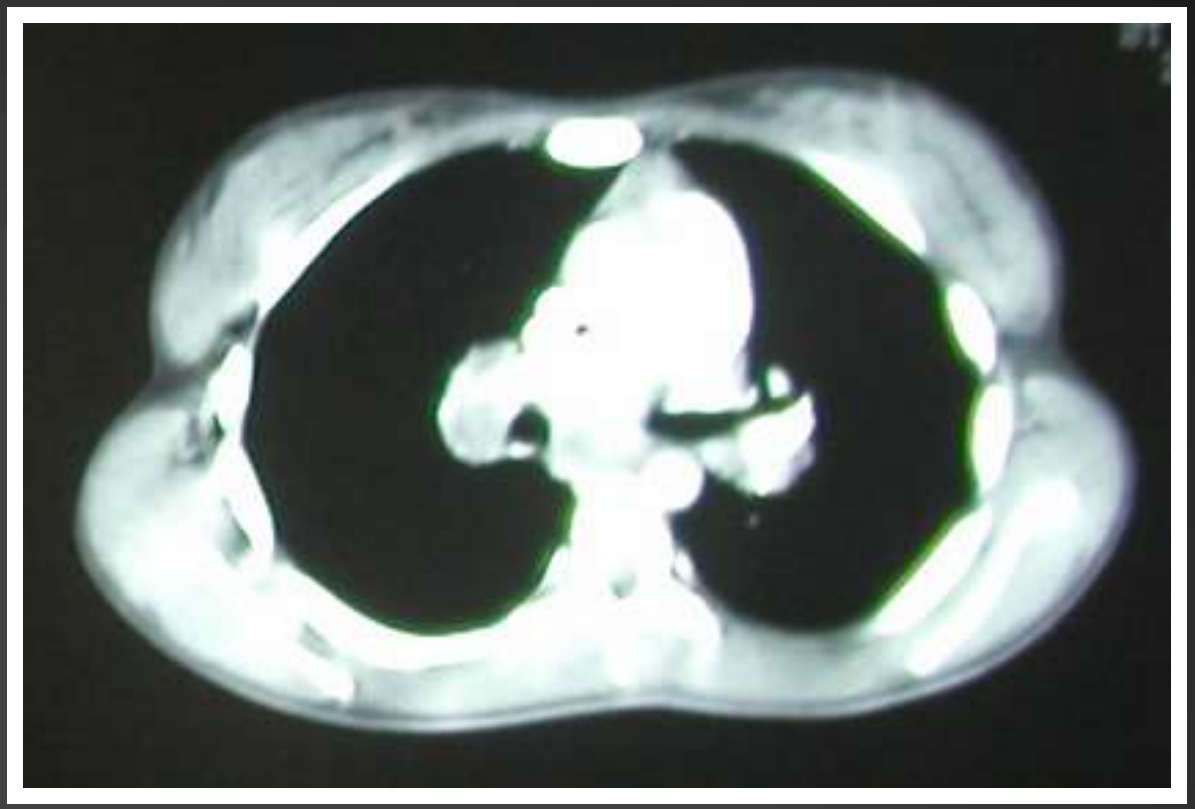

HODGKIN

Mujer de 31 años
Ensanchamiento Hiliar Bilateral

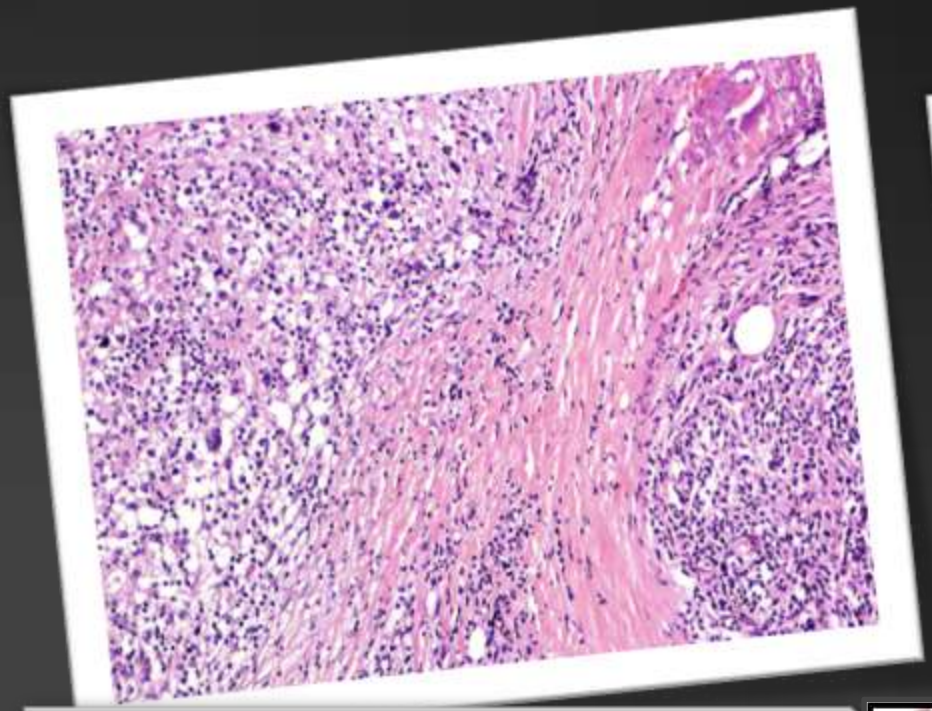

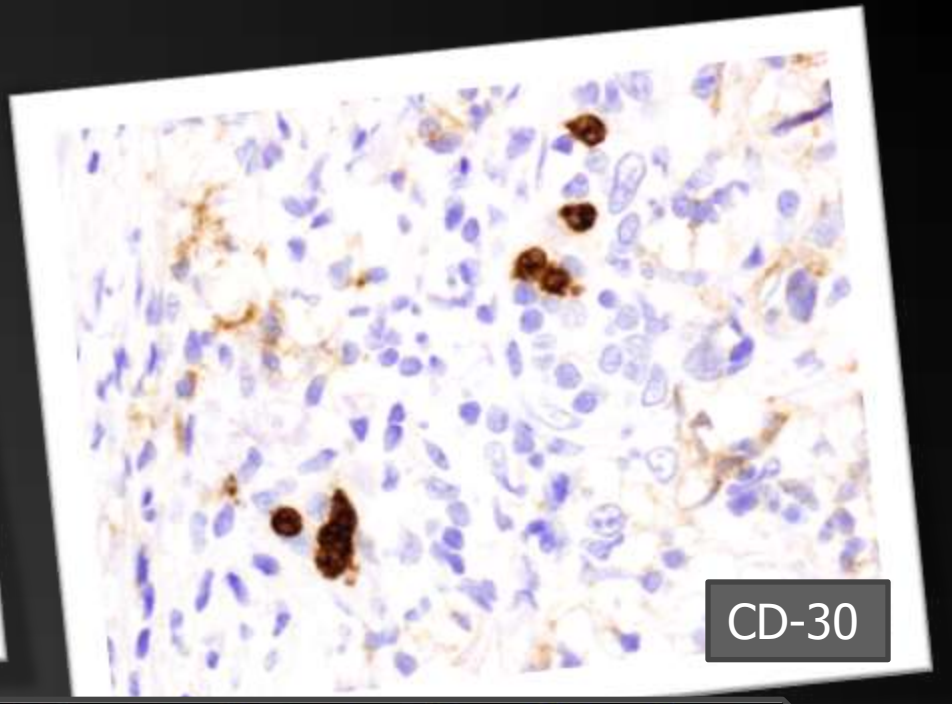
CD-30

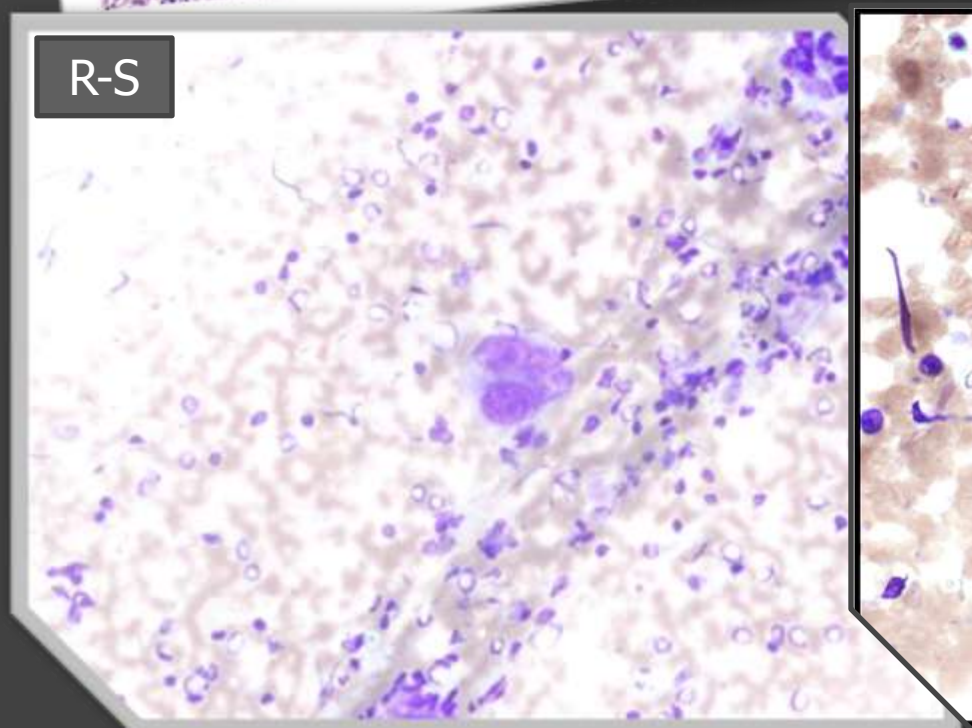
R-S

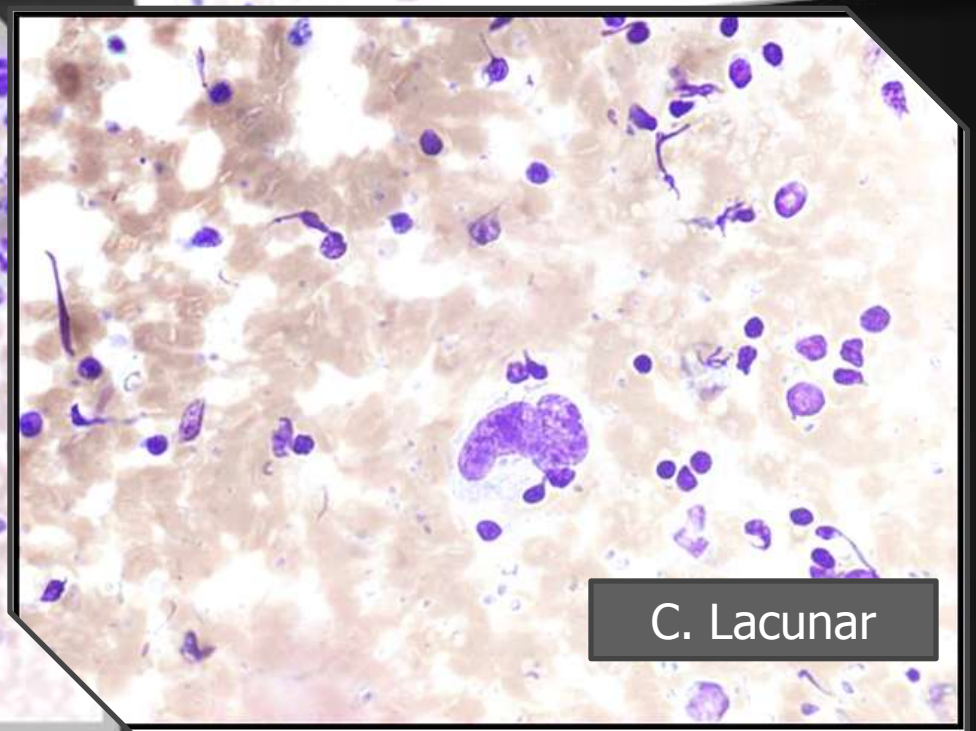
C. Lacunar

E. HODGKIN

Células similares en:

Infecciones (Mononucleosis infecciosa)
Postvacunales
Hipersensibilidad a Fármacos.
Linfomas T Anaplásicos.
Linfomas T Periféricos.
Linfomas B ricos en células T.
Carcinomas (cavum)
Melanomas.

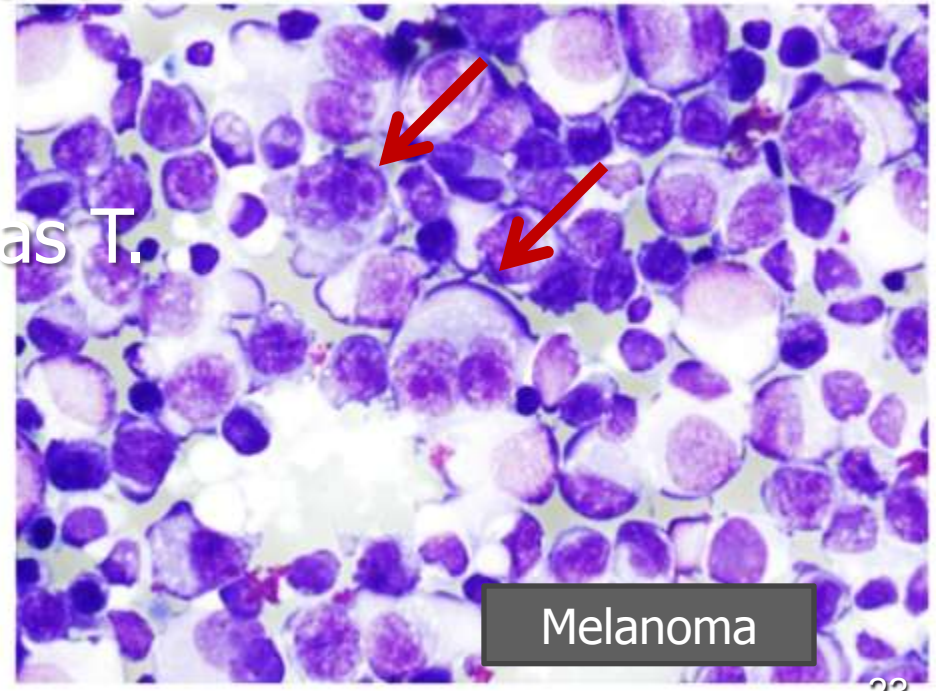

Melanoma

ESTADIAJE C. PULMON

DIFICULTADES

ESCASEZ MUESTRA

NECROSIS

DEGENERACION QUISTICA

C. ANAPLASICO
C. PEQUEÑA

Varón 63 años
Masa LSI
Adenopatías

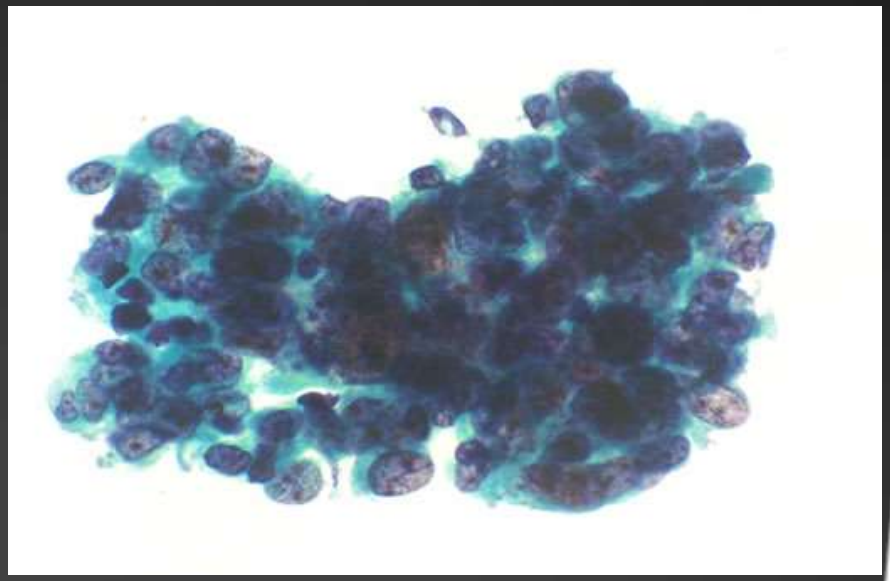

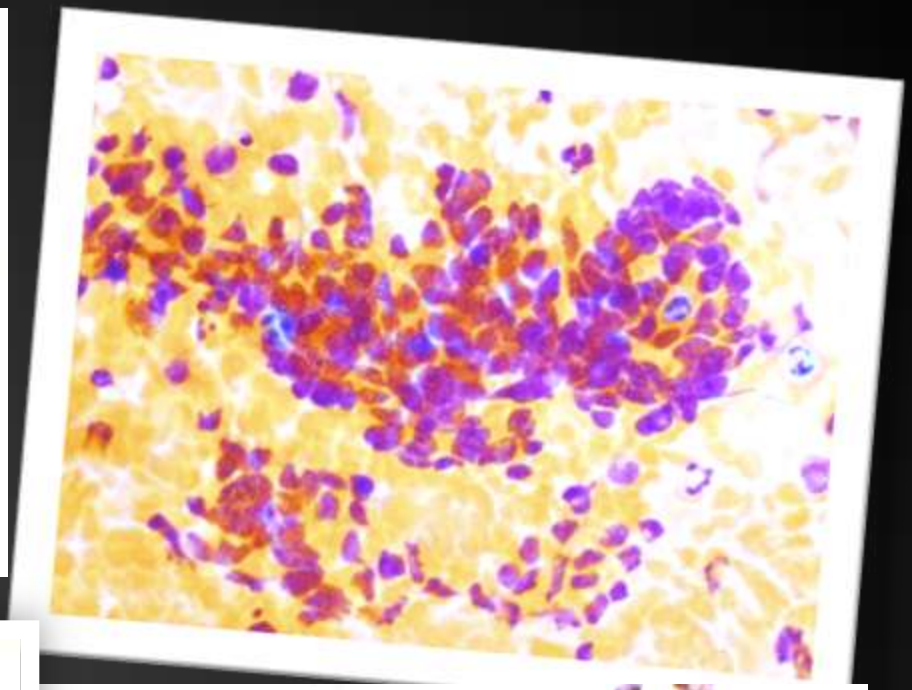

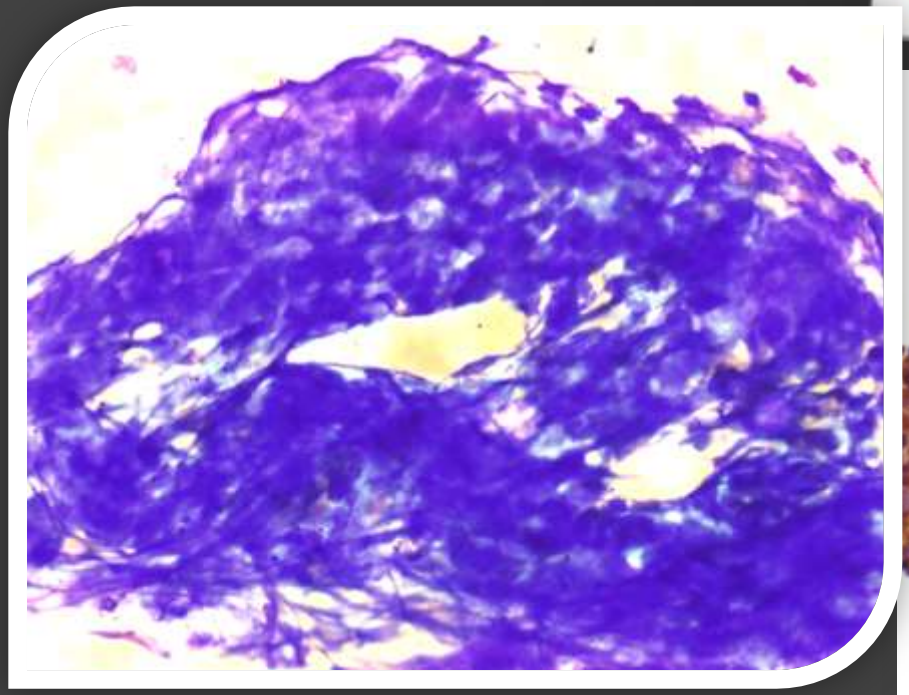

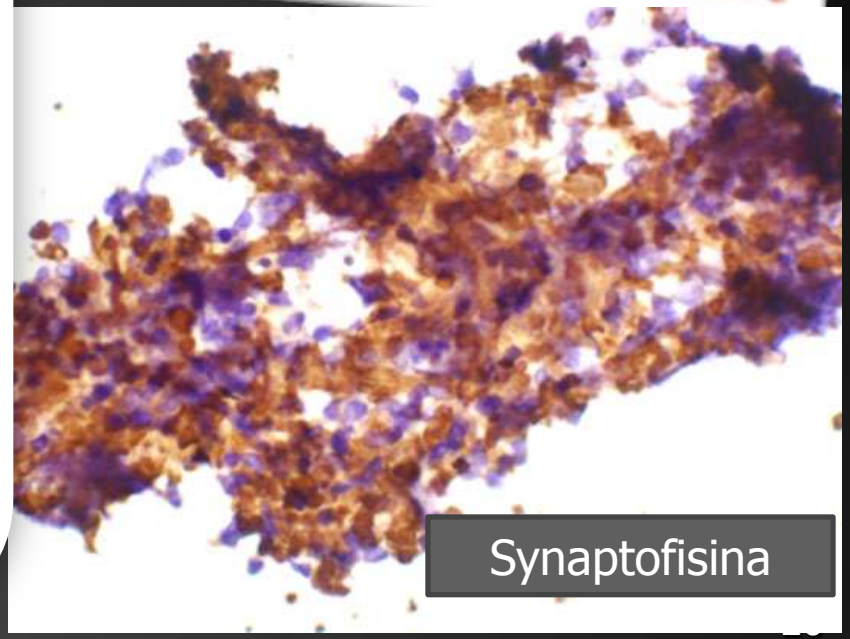
Synaptofisina

C. ANAPLÁSICO DE C. PEQUEÑAS LINFOMA

Algún acúmulo con moldeamiento

Algún núcleo agrandado

Fondo necrótico

Ausencia cuerpos linfoglandulares

C. NEUROENDOCRINO de C. GRANDES

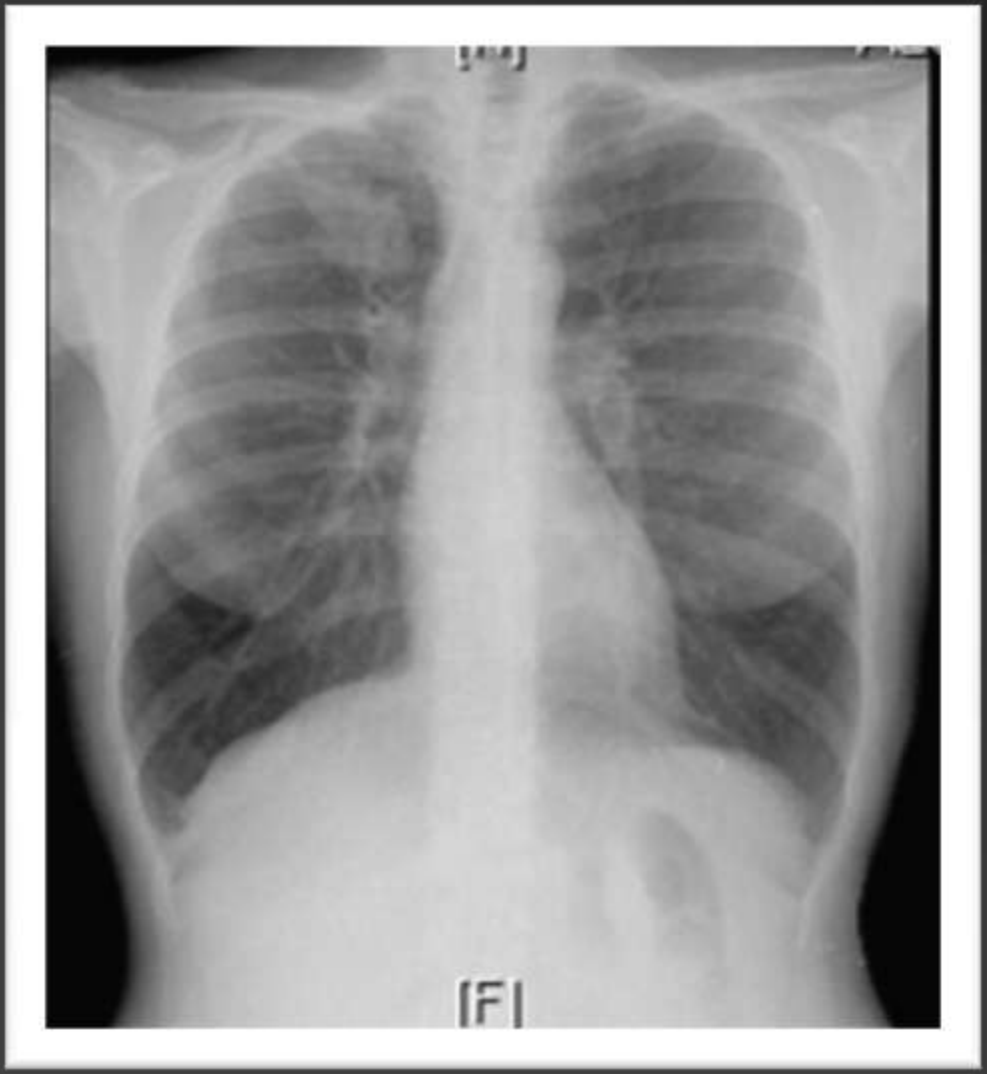

Mujer 41 años
Masa Pulmonar
Adenopatías Mediastínicas

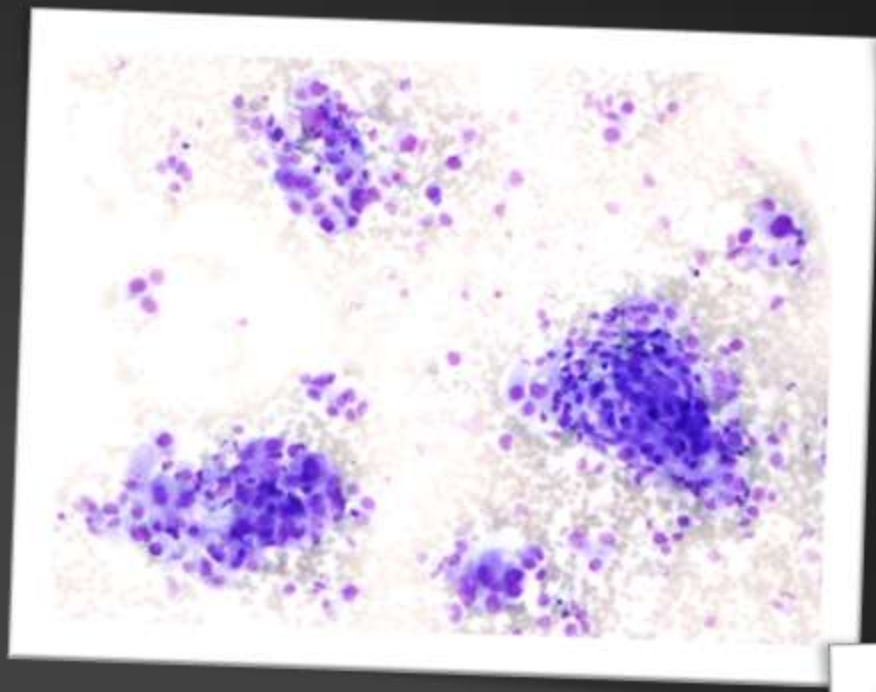

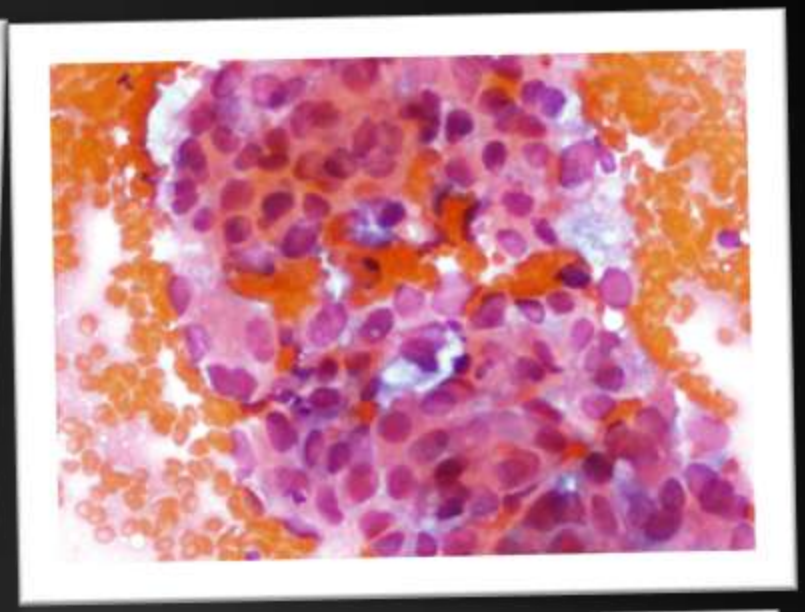

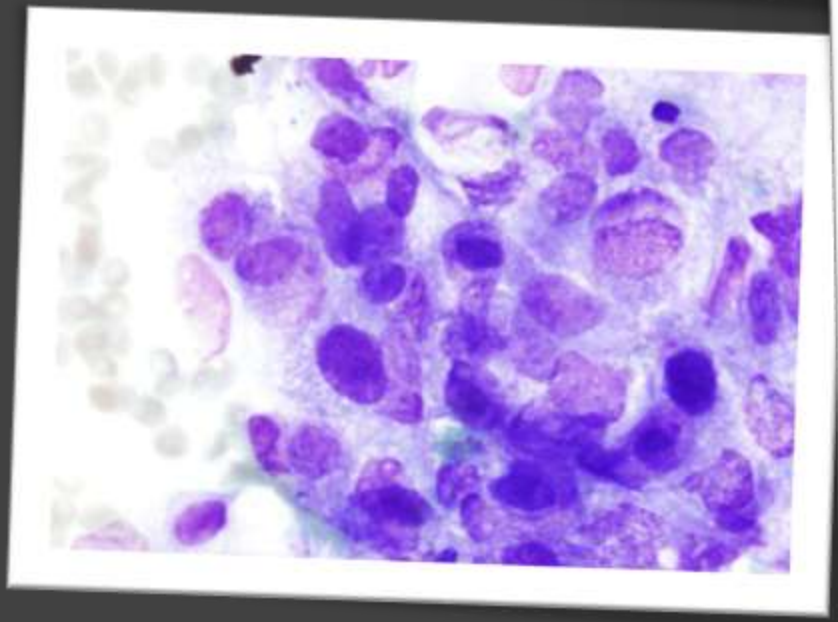

Synaptofisina

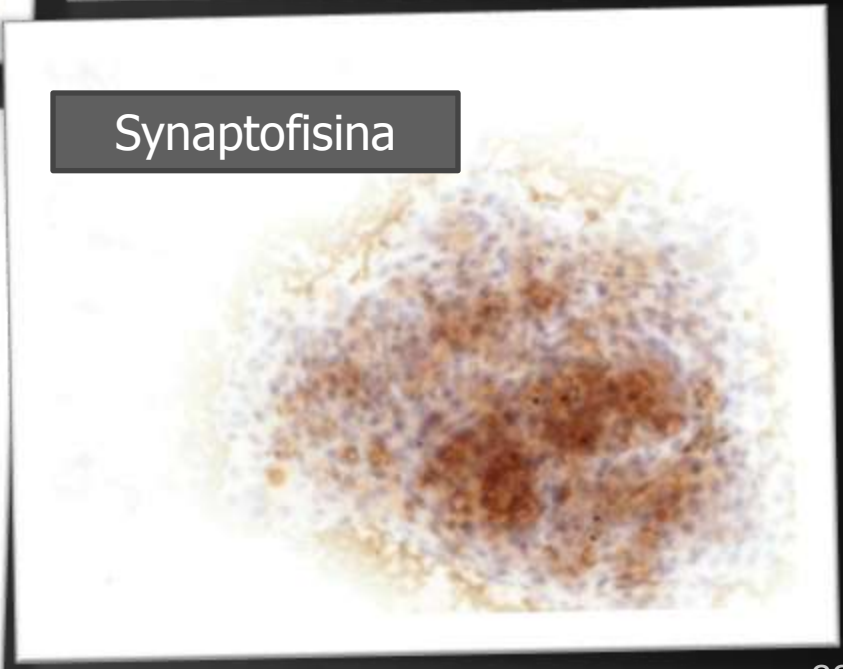

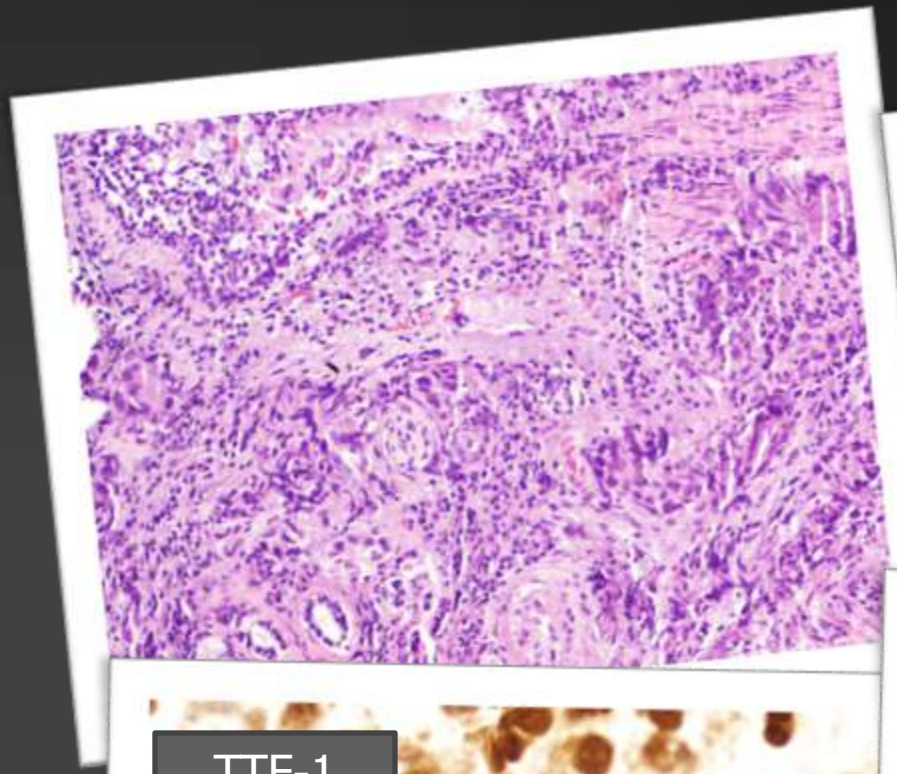

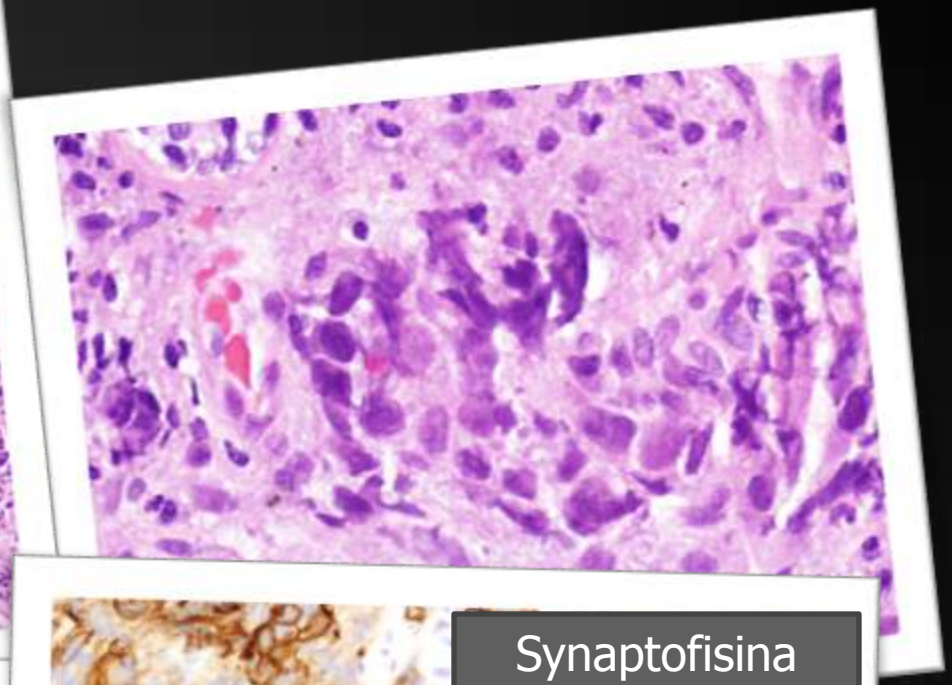

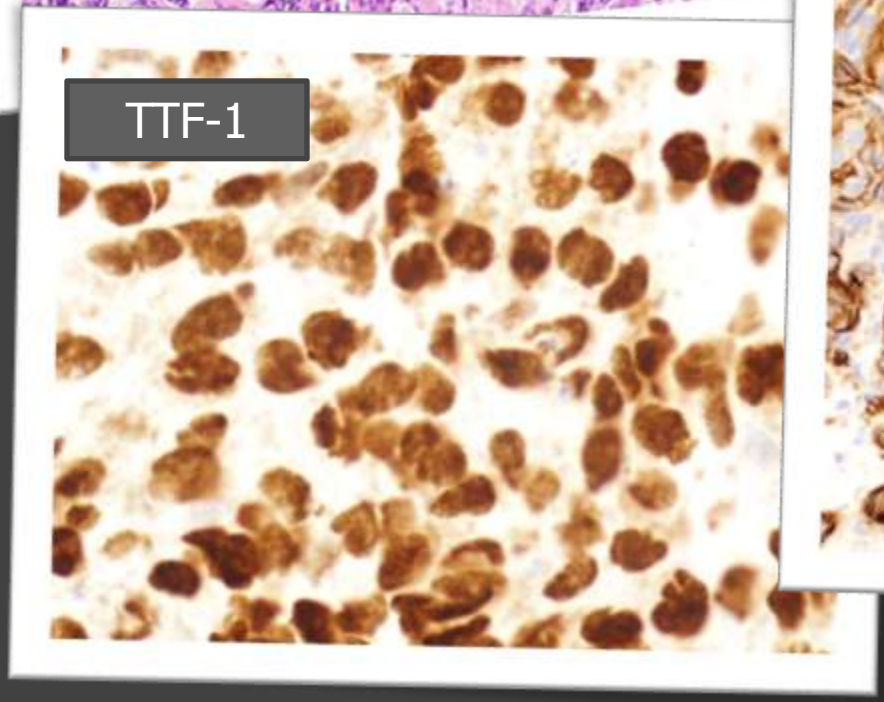
TTF-1

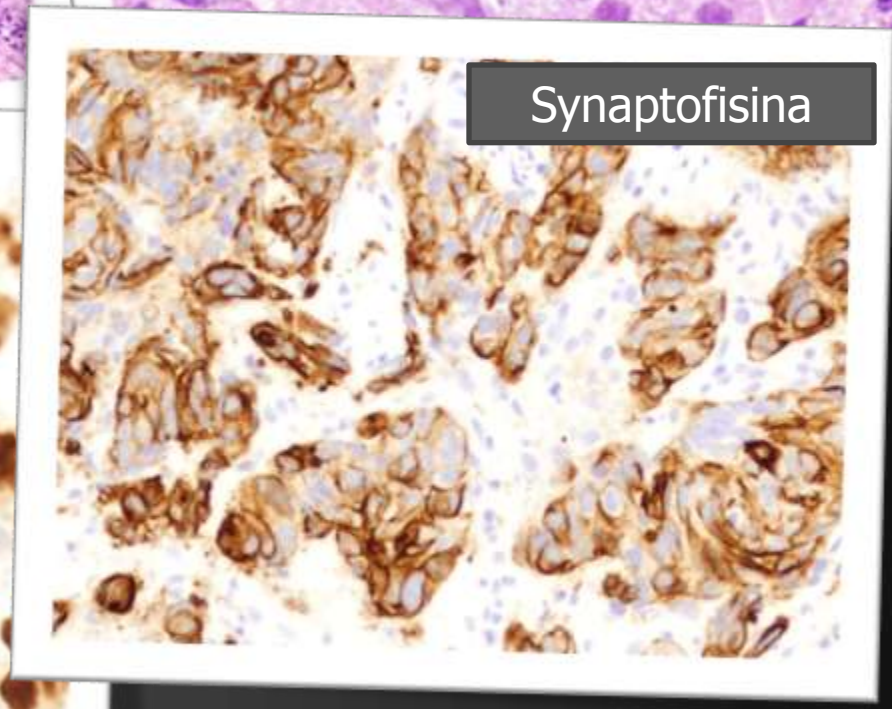
Synaptofisina

C. NEUROENDOCRINO C. GRANDE C. ANAPLÁSICO C. PEQUEÑA

Núcleo más pequeño

Nucléolo incospicuo

Escaso citoplasma

Moldeamiento nuclear más acusado

C. NEUROENDOCRINO C. GRANDE
CARCINOIDE ATÍPICO

Pleomorfismo Celular

Núcleo Vesicular

Nucléolo Prominente

C. NEUROENDOCRINO C. GRANDE ADENOCARCINOMA

Papilas

Acinos

	CARCINOMA ESCAMOSO	C. NEUROENDOCRINO CELULAS GRANDES
Ck 5/6	+	-
Ck 13	+	-
Ck 14/15	+	-
Ck 16	+	-
Ck 17	+	-
p 16	+	-
Desmocolina	+	-
Cromogronina A	-	+
Sinaptofisina	-	+
CD 56	-	+
TTF-1	-	+

METÁSTASIS GANGLIONARES

Carcinoide típico……10%

Carcinoide atípico……50%

C. Anaplásico C. pequeña……Muy frecuentes

C. Anaplásico C. grande……Frecuentes

T. NEUROENDOCRINOS

Moldeamiento nuclear

Artefacto de aplastamiento

Mitosis

Necrosis

Nucléolo variable

Ki - 67

Carcinoide típico	<2%
Carcinoide atípico	<20%
C. Anaplásico C. pequeña	60-100%
C. Neuroendocrino C. grandes	+20%

C. BASALIOIDE

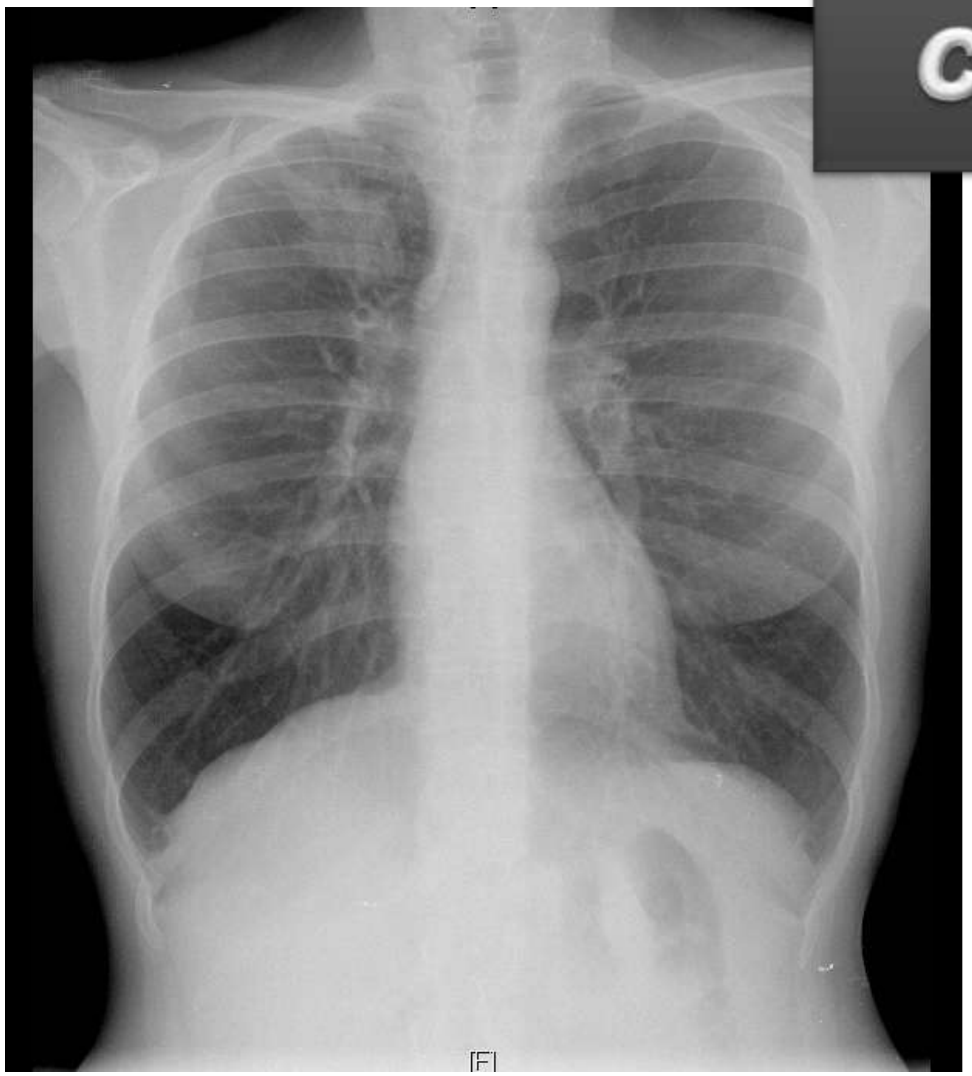

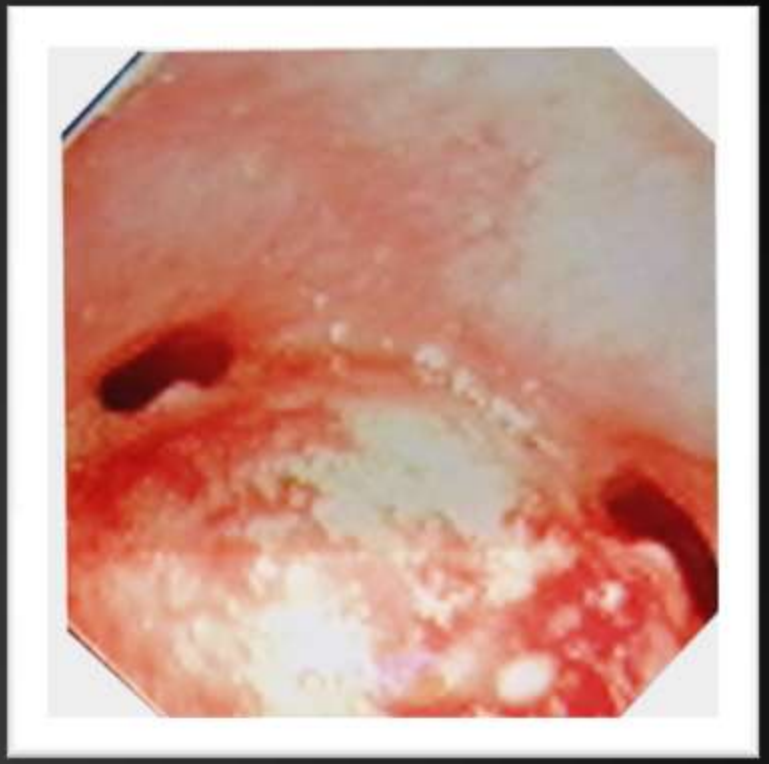

Mujer 45 años
Lesión Pulmonar

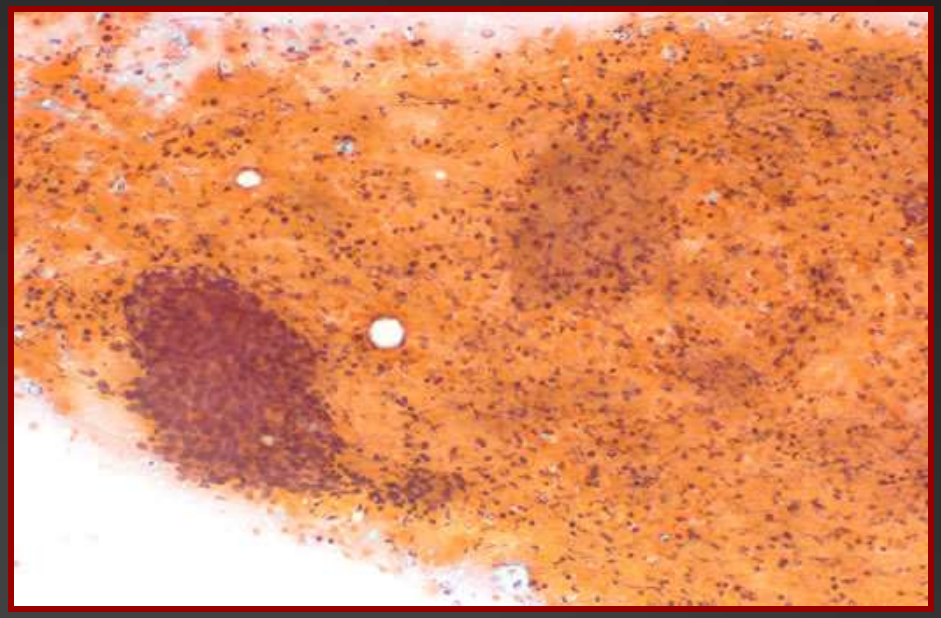

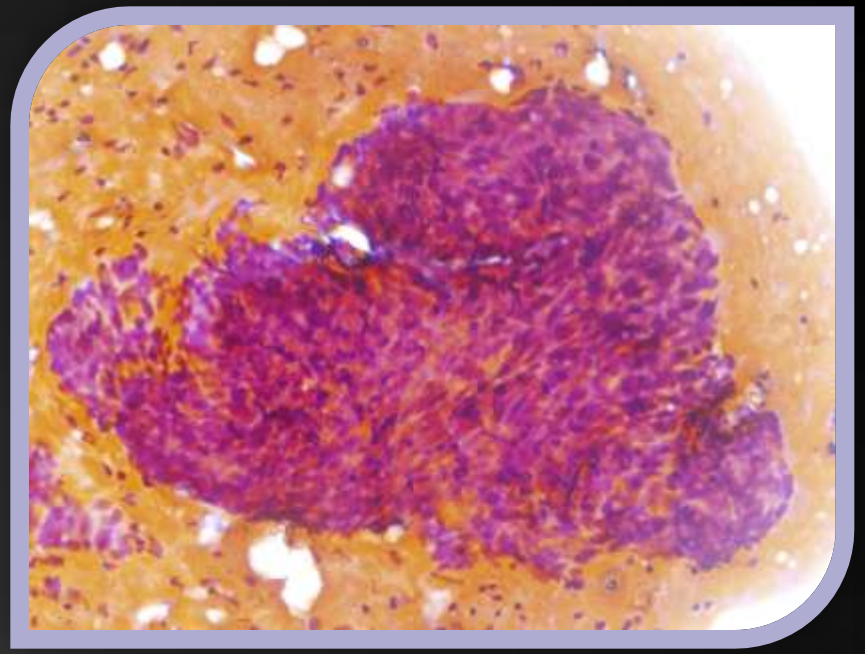

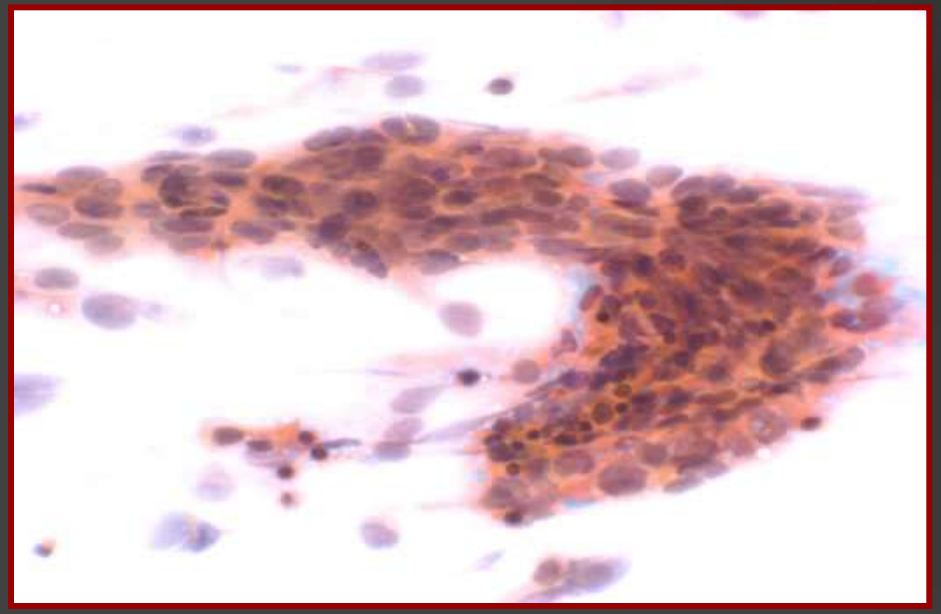

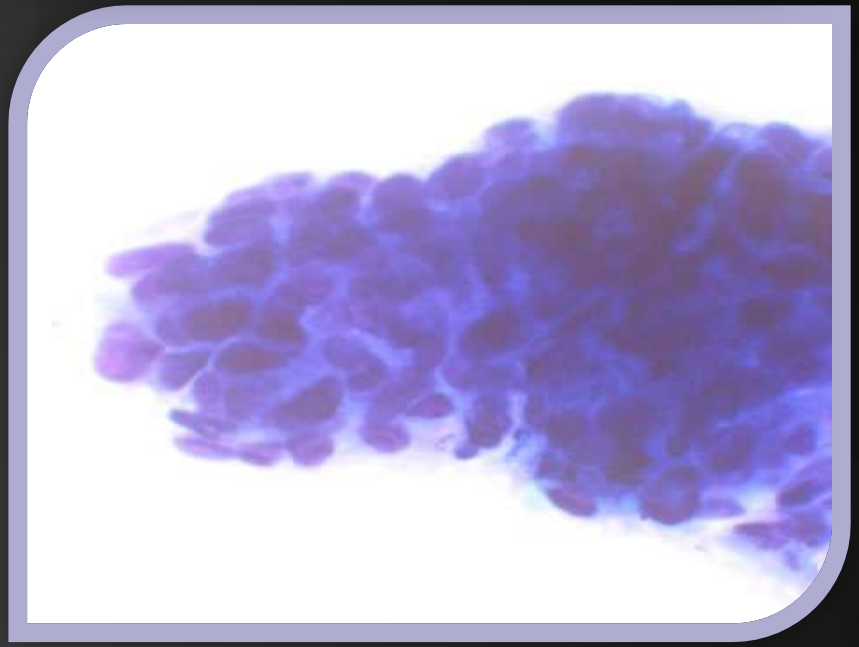

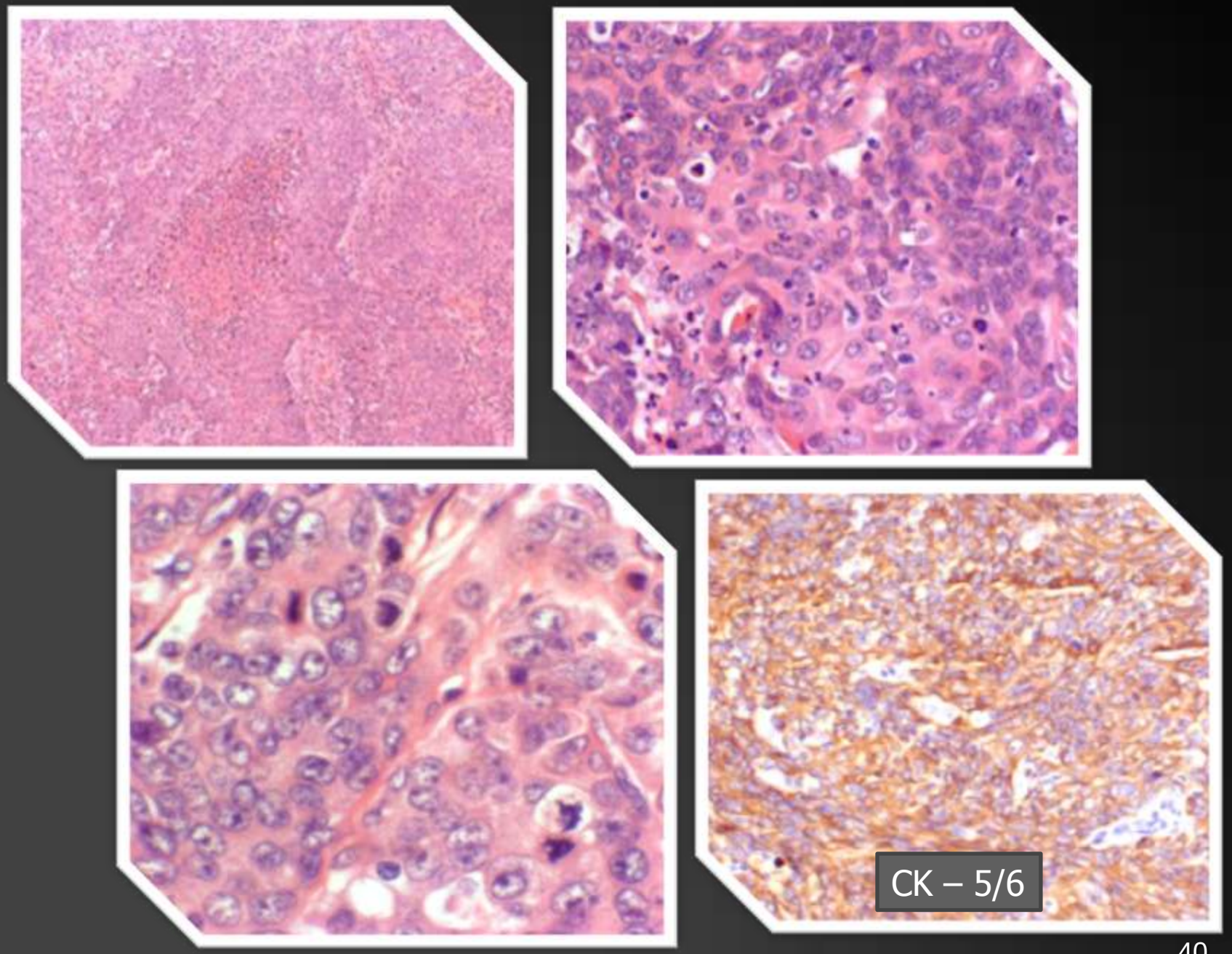
CK – 5/6

	C. BASALIOIDE	C. NEUROENDOCRINO C.GRANDE	C. ANAPLASICO C. PEQUEÑA
CD-56		+	+
Cromogranina		+	+
Sinaptofisina		+	+
34BE-12	+	-	
TTF-1	-	+	+
CK 5/6	+	-	

TUMORES NEUROENDOCRINOS / SEMEJANTES

	Linfocitos Linfomas	***Carcinoide***	***Oat-cell***	***C Neuroendocrino Células grandes***	***C. Basalioide***
Disposición	Aisladas A veces acúmulos	Aisladas, y grupos lasos Rosetas y asociadas con vasos sanguineos	Grupos Ailadas	Cohesivos	Grupos con empalizada en los bordes
Nucleo	Pequeños, redondos cromatina grumosa	Pequeños, redondos, monomorficos cromatina libre No moldeamiento	Pequeños, moldeados, pleomorficos, cromatina libre	Grande, ocasionalmente moldeamiento	Núclos oval o fusiforme, cromatima grumosa
Nucleolo	Prominente en algunos linfomas	Incospicuo	Inconspicuo	Prominente	Ausente
Citoplasma	Escaso, ausente y basófilo	Más abundante granular plasmocitoide	Escaso/ Ausente	Más abundante granular	Abundante y denso
Fondo	Cuerpos lifogranulados	Capilares ramificados. Necrosis ocasional (C. atipico)	Apoptotico y Necrotico	Apoptotico y Necrotico	A veces Necrosis

TBNA/ ULTRASONOGRAFÍA ENDOBRONQUIAL

Originalien

1999

Endobronchiale Sonographie zur Diagnostik pulmonaler und mediastinaler Tumoren

Th. Hürter und P. Hanrath

Medizinische Klinik I (Direktor: Prof. Dr. P. Hanrath) der Rheinisch-Westfälischen Technischen Hochschule Aachen

Bei 58 Patienten (48 Männern, zehn Frauen, mittleres Alter 59 [29–76] Jahre) mit gesicherten malignen mediastinalen oder pulmonalen Tumoren wurde im Rahmen einer Bronchoskopie eine endobronchiale Sonographie mit 6,2- oder 9-F-Ultraschallkathetern durchgeführt. In 50 Fällen war die endoluminale Sonographie von der Trachea bis zu Bronchien von 2 mm Durchmesser möglich. Bei fünf Patienten mit kleinen peripheren Rundherden konnte das Tumorgewebe sonographisch nicht dargestellt werden; in drei Fällen war der Tumor mit der Katheterson de nicht passierbar. Die Sonographie zeigte einen dreischichtigen Aufbau der Bronchialwand, entsprechend den histologischen Gewebsschichten Mucosa, Knorpel und Adventitia. Pulmonalarterien wurden an echofreien Lumen und den pulsatorischen Kaliberschwankungen erkannt. Tumoren sowie Lymphknoten waren echoarm und konnten dadurch von der echoreichen Bronchialwand abgegrenzt werden. Aus den Ergebnissen der endobronchialen Sonographie ergaben sich unmittelbare Konsequenzen: In zwei Fällen wurde auf eine Laser-Therapie verzichtet, weil im Bereich der Stenose eine größere Pulmonalarterie lag. In drei Fällen wurden rein intramural oder peribronchial wachsende Malignome nachgewiesen, die der endoskopischen Inspektion entgangen waren. Nach diesen ersten Erfahrungen stellt die endobronchiale Sonographie eine vielversprechende Ergänzung der bisherigen bronchoskopischen Untersuchungsverfahren dar.

Endobronchial sonography in the diagnosis of pulmonary and mediastinal tumours

Endobronchial sonography was performed during bronchoscopy in 58 patients (48 males and 10 females; mean age 59 [29–76] years) with confirmed pulmonary or mediastinal tumour using a 6.2 or 9F ultrasound catheter. The procedure was successfully performed in 50 patients from the trachea down to the smallest bronchi (of 2 mm diameter). Tumour tissue was not visualised in five patients with small peripheral carcinomas. In three patients the catheter probe could not be passed through the tumour region. The method provided a three-dimensional image of the bronchial wall, corresponding to the histological tissue layers of mucosa, cartilage and adventitia. Pulmonary arteries were identified by the echo-free lumen and pulsatile oscillations in calibre. Tumours and lymph-nodes were echo-poor and could thus be distinguished from the echo-rich bronchial wall. Several consequences arose from these findings: laser treatment was not proceeded with in two cases, because a fairly large pulmonary artery lay near the stenosis; in three cases malignant tumours were recognized to lie either entirely intramurally or peribronchially, which had not been seen on bronchoscopy alone. It is concluded from these preliminary observations that endobronchial sonography is a highly promising addition to conventional bronchoscopy.

Die intrakavitäre Sonographie wurde entwickelt, um Organ- und Gewebestrukturen darzustellen, die wegen ihrer anatomischen Lage durch andere diagnostische Verfahren nur unzureichend abgebildet werden. Durch den direkten Organkontakt können hochfrequente Ultraschallsonden eingesetzt werden, die eine große Detailauflösung ermöglichen. Die Endosonographie des oberen und unteren Gastrointestinaltraktes erlaubt eine Analyse muraler und extramuraler Organveränderungen [6, 7, 9, 11, 17, 19–21]. Ein ähnlicher Weg wurde mit der transösophagealen Echokardiographie beschritten, die einen neuen sonographischen Zugang zum Herzen und der thorakalen Aorta ohne Interposition von

Dtsch. med. Wschr. 115 (1990), 1899–1903
© Georg Thieme Verlag Stuttgart · New York

Hurter T. Hanrath P

Kazuhiro Yasufuku

Real-time Endobronchial Ultrasound-Guided Transbronchial Needle Aspiration of Mediastinal and Hilar Lymph Nodes*

Kazuhiro Yasufuku, MD; Manabu Chiyo, MD; Yasuo Sekine, MD; Prashant N. Chhajed, MD, FCCP; Kiyoshi Shibuya, MD; Toshihiko Iizuka, MD; and Takehiko Fujisawa, MD

Study objectives: **Although various techniques are available for obtaining pathology specimens from the mediastinal lymph nodes, including conventional bronchoscopic transbronchial needle aspiration (TBNA), transesophageal ultrasonography-guided needle aspiration, and mediastinoscopy, there are limitations to these techniques, which include low yield, poor access, need for general anesthesia, or complications. To overcome these problems, we undertook the current study to evaluate the clinical utility of the newly developed ultrasound puncture bronchoscope to visualize and perform real-time TBNA of the mediastinal and hilar lymph nodes under direct endobronchial ultrasonography (EBUS) guidance.**

Design: **Prospective patient enrollment.**

Setting: **University teaching hospital.**

Patients: **From March 2002 to September 2003, 70 patients were included in the study.**

Interventions: **The new convex probe (CP) EBUS is integrated with a convex scanning probe on its tip with a separate working channel, thus permitting real-time EBUS-guided TBNA. The indications for CP-EBUS were the diagnosis of mediastinal and/or hilar lymphadenopathy for known or suspected malignancy. Lymph nodes and the surrounding vessels were first visualized with CP-EBUS using the Doppler mode. The dimensions of the lymph nodes were recorded, followed by real-time TBNA under direct EBUS guidance. Final diagnosis was based on cytology, surgical results, and/or clinical follow-up.**

Results: **All lymph nodes that were detected on the chest CT scan could be visualized using CP-EBUS. In 70 patients, CP-EBUS-guided TBNA was performed to obtain samples from mediastinal lymph nodes (58 nodes) and hilar lymph nodes (12 nodes). The sensitivity, specificity, and accuracy of CP-EBUS-guided TBNA in distinguishing benign from malignant lymph nodes were 93.7%, 100%, and 97.1%, respectively. The procedure was uneventful, and there were no complications.**

Conclusions: **Real-time CP-EBUS-guided TBNA of mediastinal and hilar lymph nodes is a novel approach that is safe and has a good diagnostic yield. This new ultrasound puncture bronchoscope has an excellent potential for assisting in safe and accurate diagnostic interventional bronchoscopy.** ***(CHEST 2004; 126:122–128)***

Key words: bronchoscopy; endobronchial ultrasound; lung cancer; lymph node metastasis; staging; transbronchial needle aspiration

Abbreviations: CP = convex probe; EBUS = endobronchial ultrasonography; TBNA = transbronchial needle aspiration; US = ultrasonography

Various techniques are available for obtaining pathology specimens from the mediastinal lymph nodes, including mediastinoscopy, CT-guided percutaneous needle aspiration, conventional bronchoscopic transbronchial needle aspiration (TBNA), CT-guided TBNA, and transesophageal ultrasonography (US)-guided needle aspiration.[1–4] All of these techniques have some limitations, which include variation in yield, complications, poor access to some lymph nodes, need for general anesthesia, exposure to radiation, or the referral to a service that offers the specialized procedure.[3,5] Endobronchial ultrasonography (EBUS) using a radial probe through the working channel of the flexible bronchoscope has been used to identify mediastinal and hilar lymph nodes.[6] In addition, EBUS guidance has recently

PUNCIÓN TRANSBRONQUIAL/ ULTRASONOGRAFÍA ENDOBRONQUIAL

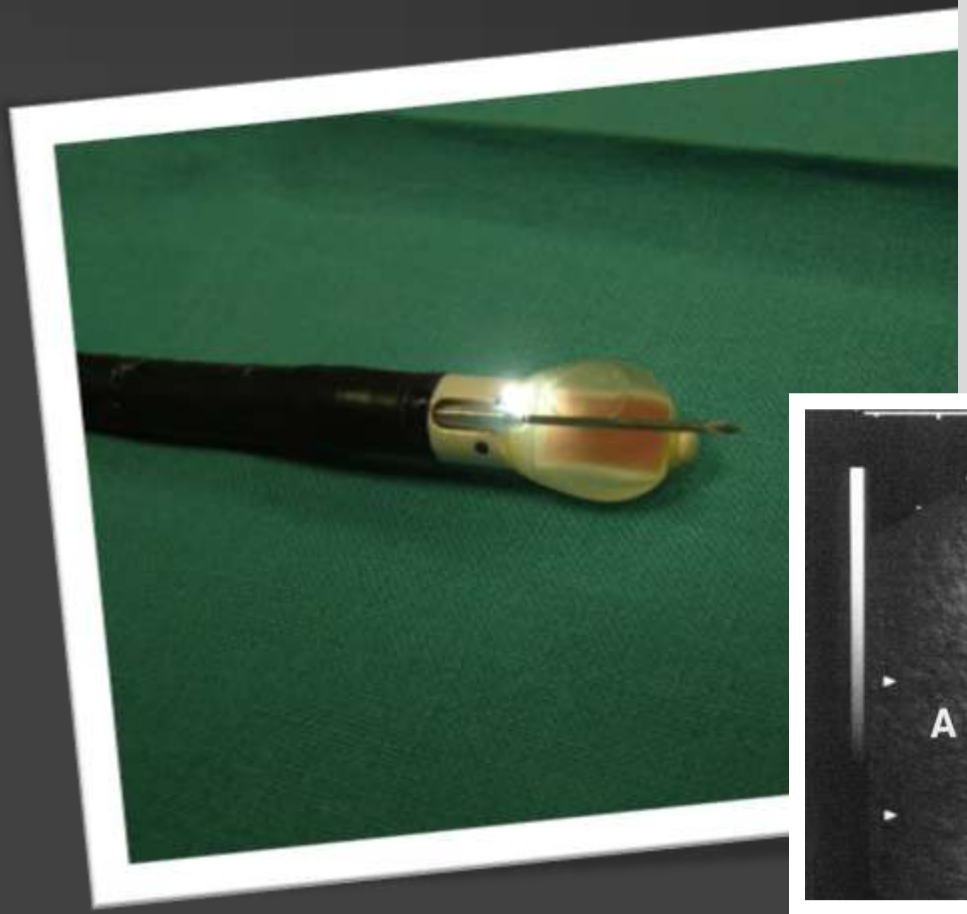

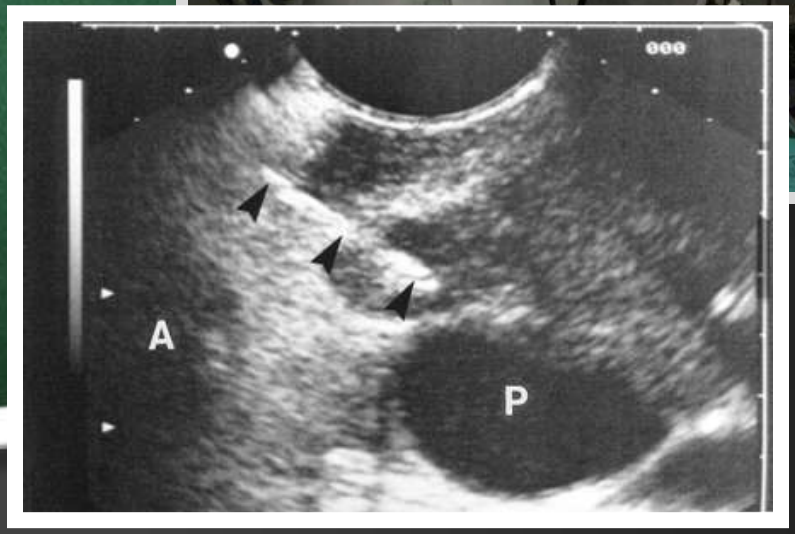

S. LINEAL

TIEMPO REAL

SENSIBILIDAD

Krasnik M

Thorax 2003; 58: 1083-6.

Rintoul RC

Eur Respir J 2005; 25: 416-21.

Herth FJ

Eur Respir J 2006; 28: 910-4.

Yasufuku K

Chest 2006; 130: 710-8.

88 – 95 %

SENSIBILIDAD / ASPIRACIONES

1ª Aspiración ---------- 68.9%
2ª Aspiración ---------- 83.7%
3ª Aspiración ---------- 95.3% 1 hora

Lee HS et al

Chest 2008; 134: 368-374.

RE - ESTADIAJE

- Especificidad 100%
- Sensibilidad 76%

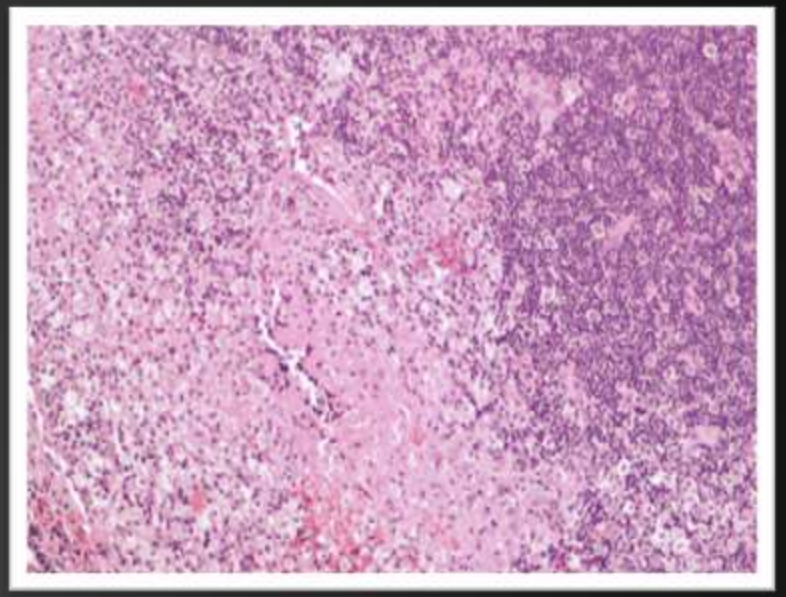

Necrosis
Fibrosis

Herth F.J.F

J Clin Oncol 2008; 36: 3346-3350.

GANGLIOS MEDIASTÍNICOS

G. M. ALTOS
- 1 M. más altos (1R y 1L)
- 2 Paratraqueales superiores (2 R y 2 L)
- 3 Prevasculares (3a) y retrotraqueales (3p)
- 4 Paratraqueales inferiores (4R y 4 L)

G. AÓRTICOS
- 5 Subaórticos (ventana aortopulmonar)
- 6 Para-aórticos (aorta ascendente)

G. M. INFERIORES
- 7 Subcarínico
- 8 Paraesofágico
- 9 Del ligamento pulmonar

GANGLIOS INTRAPULMONARES

- 10 Hiliar (10 R y 10 L)
- 11 Interlobar (11 R y 11 L)
- 12 Lobar (12 R y 12 L)
- 13 Segmentarios (13 R y 13 L)
- 14 Subsegmentarios (14 R y 14 L)

Regional Lymph Node Classification for Lung Cancer Staging*

Clifton F. Mountain, MD, FCCP, and Carolyn M. Dresler, MD, FCCP

Recommendations for classifying regional lymph node stations for lung cancer staging have been adopted by the American Joint Committee on Cancer (AJCC) and the Union Internationale Contre le Cancer. The objective was to unify the two systems that have been in common use for the past 10 years; that is, the schema advocated by the AJCC, adapted from the work of Tsuguo Naruke, and the schema advocated by the American Thoracic Society and the North American Lung Cancer Study Group. Anatomic landmarks for 14 hilar, intrapulmonary, and mediastinal lymph node stations are designated. This classification provides for consistent, reproducible, lymph node mapping that is compatible with the international staging system for lung cancer. It is applicable for clinical and surgical-pathologic staging. (CHEST 1997; 111:1710-17)

Key words: lung cancer; lymph node classification; lymph node mapping; lymph nodes; staging; survival rates

Abbreviations: AJCC=American Joint Committee on Cancer; ATS=American Thoracic Society; cN=status of lymph nodes according to all diagnostic and evaluative information obtained prior to the institution of treatment or decision for no treatment; LCSG=Lung Cancer Study Group [National Cancer Institute North American Cooperative Lung Cancer Study Group]; N=regional lymph nodes; pN=status of lymph nodes according to surgical-pathologic information obtained from resected specimens; TNM=subset describing the extent of disease in terms of the T compartment, primary tumor, the N compartment, regional lymph nodes, and the M compartment, distant metastasis

The status of regional lymph nodes is a major factor for staging, assigning treatment, and evaluating treatment efficacy in patients with lung cancer. Consistent, reproducible classification or mapping of these lymph nodes is essential for designing clinical research studies that are needed to fully understand the implications of lymphatic metastasis. Comparative studies of prognostic factors that influence the metastatic process will be reliable only if they are based on reproducible classification. The objective of the present recommendations for classifying mediastinal, hilar, and intrapulmonary lymph nodes was to combine the features of two systems[1,2] used over the past 10 years into a single schema that is compatible with internationally accepted staging definitions for the TNM (T=primary tumor, N=regional lymph nodes, M=distant metastasis) categories.[3,4]

For editorial comment see page 1498
For related material see page 1710

LYMPH NODE MAPPING

The recommendations for classifying regional lymph nodes for lung cancer staging are shown in Figure 1 with accompanying definitions in Table 1. This schema was adopted by the American Joint Committee on Cancer (AJCC) and the Prognostic Factors TNM Committee of the Union Internationale Contre le Cancer at the 1986 annual meetings of each of these organizations (see Appendix for participants and organizational representation). The diagram and definitions unify in a single system the features of the lymph node classification developed by Naruke and coworkers,[5-7] which was based on data and was approved by the AJCC, and the schema advocated by the American Thoracic Society and the North American Lung Cancer Study Group (ATS/LCSG).[8-10] Differences in classifying the lymph node stations according to the two systems resulted in confusion in the interpretation of end results.[11] The AJCC and ATS lymph node classifications are similar, except for the ATS stations 10L (designated left peribronchial nodes), and 10R (designated right tracheobronchial nodes) vs Naruke station 10 (designated hilar nodes) and Naruke station 4 (designat-

*From the Division of Cardiothoracic Surgery (Dr. Mountain), The University of California Medical Center at San Diego, and the Department of Surgical Oncology (Dr. Dresler), Fox Chase Cancer Center, Philadelphia.
Supported by the Clifton F. Mountain Foundation, including an educational grant from Bristol Myers Squibb, Oncology Division.
Manuscript received February 2, 1987; revision accepted March 27.

1710

Special Report

Mountain y Dresler

EBUS

1	8
2	
3	9
4	
7	5
10	
11	6
12	

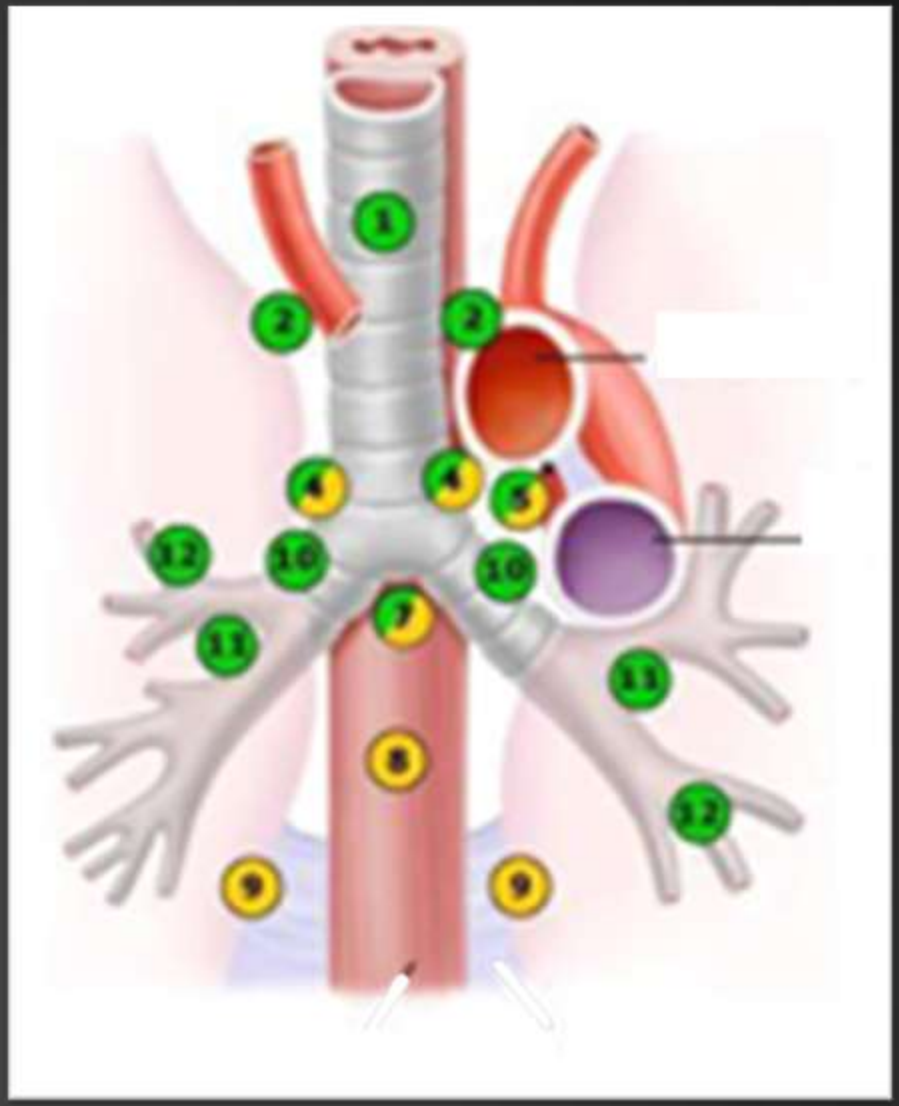

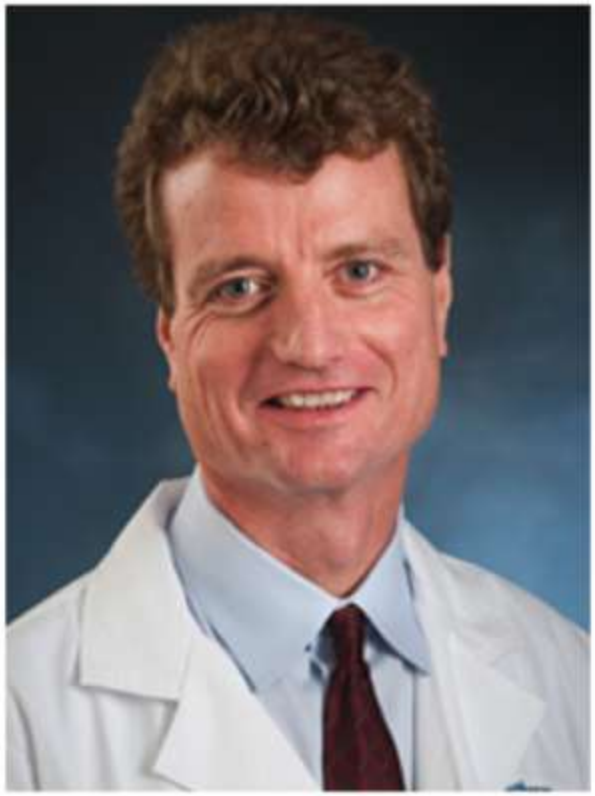

Maurits J. Wiersema, MD

Gastrointest Endosc. 1994 Nov-Dec;40(6):700-7.

Endosonography-guided real-time fine-needle aspiration biopsy.

Wiersema MJ, Kochman ML, Cramer HM, Tao LC, Wiersema LM.

Department of Medicine, St. Vincent Hospitals and Health Care Center, Indianapolis, Indiana.

Abstract

Twenty-six patients were prospectively evaluated with endosonography-guided real-time fine-needle-aspiration biopsy. This cohort comprised 14 patients with a pancreatic mass revealed by CT or a stricture of the main pancreatic duct seen at ERCP, 7 patients with mediastinal lymphadenopathy, 3 patients with extrapancreatic abdominal masses, and 2 patients with subepithelial or infiltrative lesions. Endosonography-guided real-time fine-needle-aspiration biopsy was diagnostic in 18 of 20 patients in whom surgical confirmation was available or in whom malignancy was found and confirmed by clinical follow-up (accuracy of 90%). In the subgroup of patients with pancreatic lesions, 3 had previously undergone nondiagnostic CT-guided fine-needle-aspiration biopsy and 2 did not have evidence of a mass by CT. Real-time fine-needle-aspiration biopsy was diagnostic for malignancy in 4 of these individuals. In the 7 patients with mediastinal lymph nodes, 2 had nondiagnostic transbronchial biopsy and 2 had no evidence of mediastinal lymphadenopathy by CT scan. Endosonography-guided real-time fine-needle-aspiration biopsy diagnosed malignancy in both individuals with nondiagnostic transbronchial studies and was able to identify mediastinal lymphadenopathy in the 2 patients with negative CT scans (malignancy confirmed with real-time fine-needle-aspiration biopsy in 1). Overall, in 9 of 10 lesions in which visualization by CT was not possible (5), CT-guided fine-needle aspiration was unsuccessful (3), or prior nonsurgical biopsy techniques were unsuccessful (2), real-time fine-needle-aspiration biopsy was diagnostic.(ABSTRACT TRUNCATED AT 250 WORDS)

PMID: 7859968 [PubMed - indexed for MEDLINE]

USE

5
7
8
9

2-L
4-L

2-R
4-L

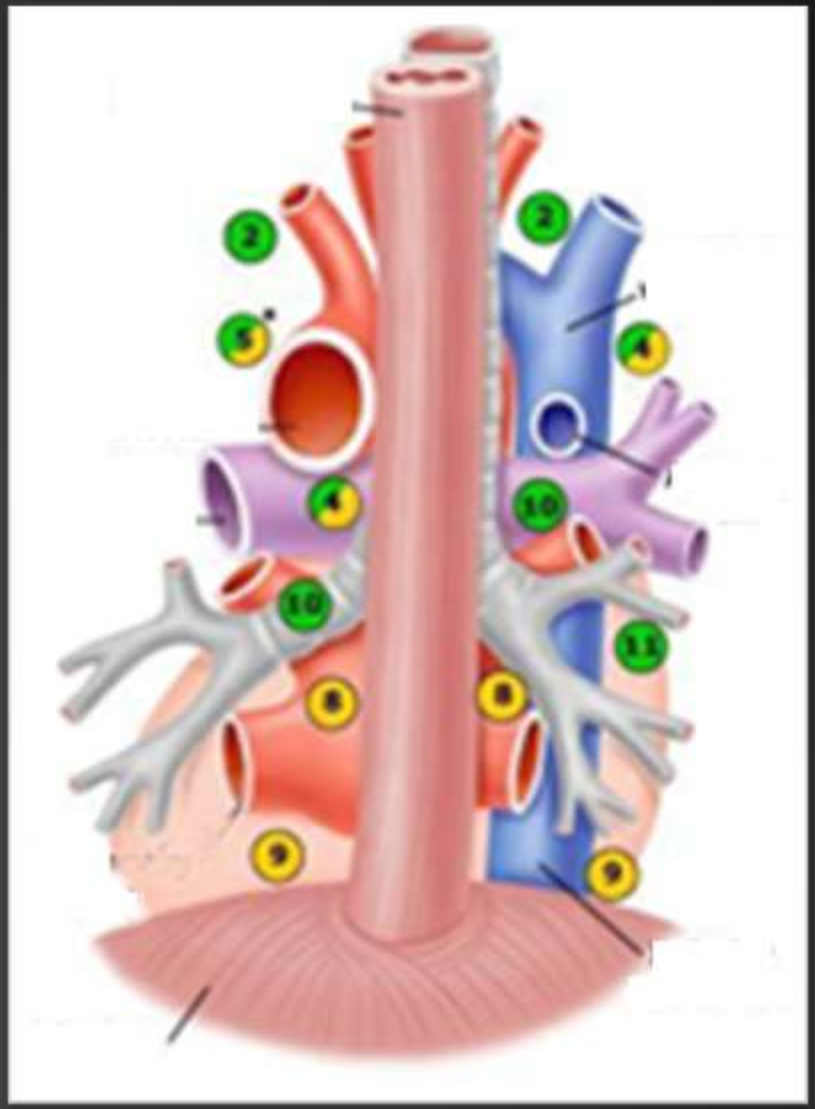

MEDIASTINOSCOPIA

2-R	8
2-L	9
4-R	5
4-L	6
1	
3	
7	

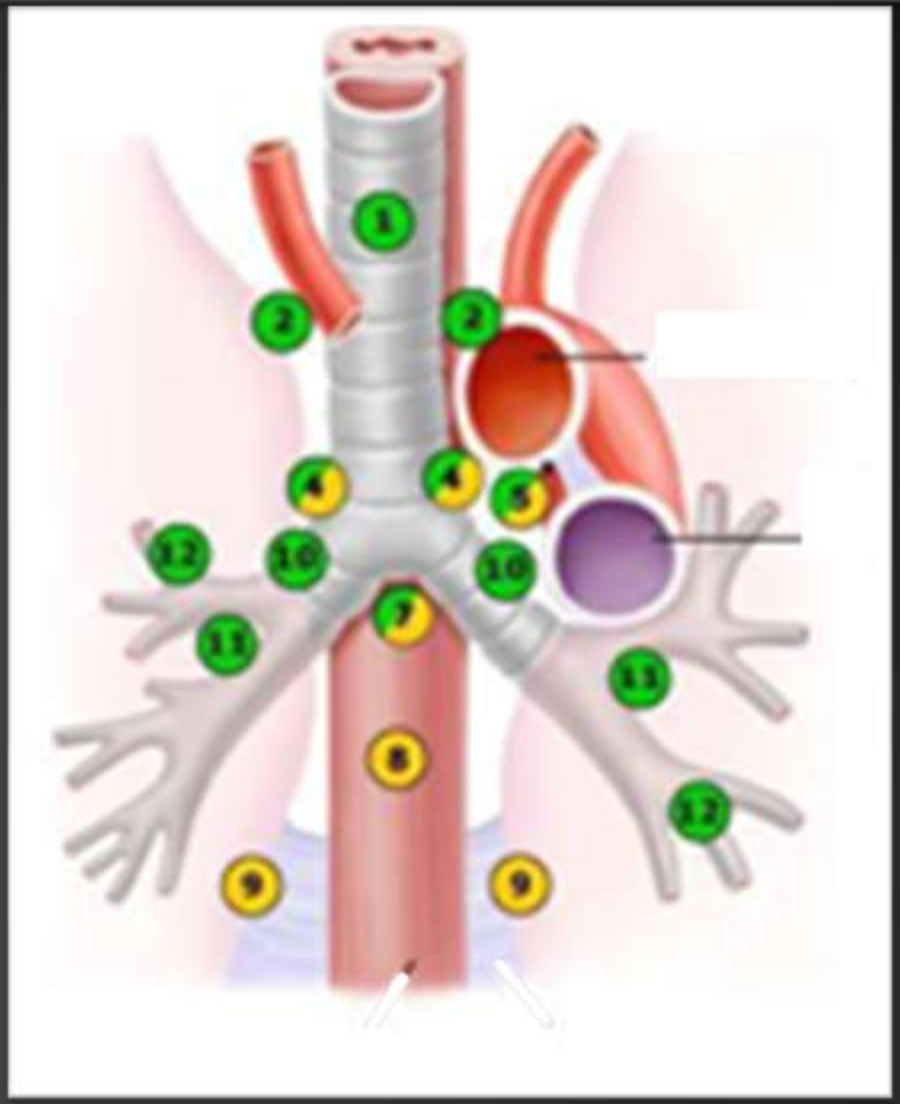

Sensibilidad 80 % Falsos negativos 10%

MEDIASTINOSCOPIA

Menos Estaciones Ganglionares

Anestesia General ----- Internamiento

Extirpación Parcial del Ganglio

Complicaciones (2%)

- Sangrado
- N. Recurrente
- Conducto Torácico

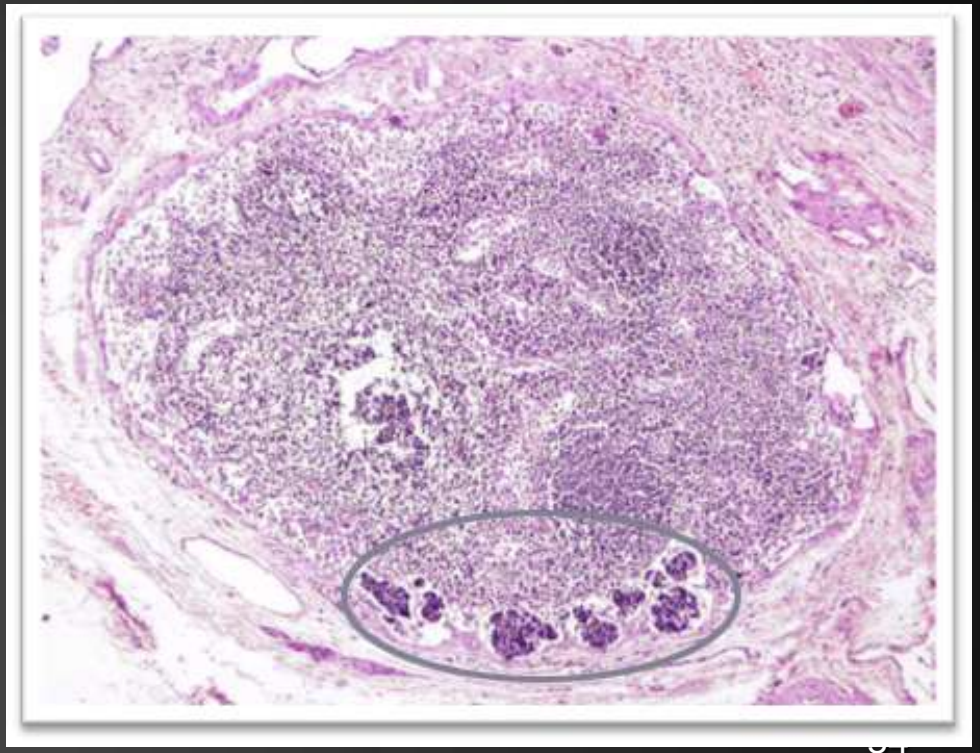

MEDIASTINOSCOPIA

EBUS / EUS

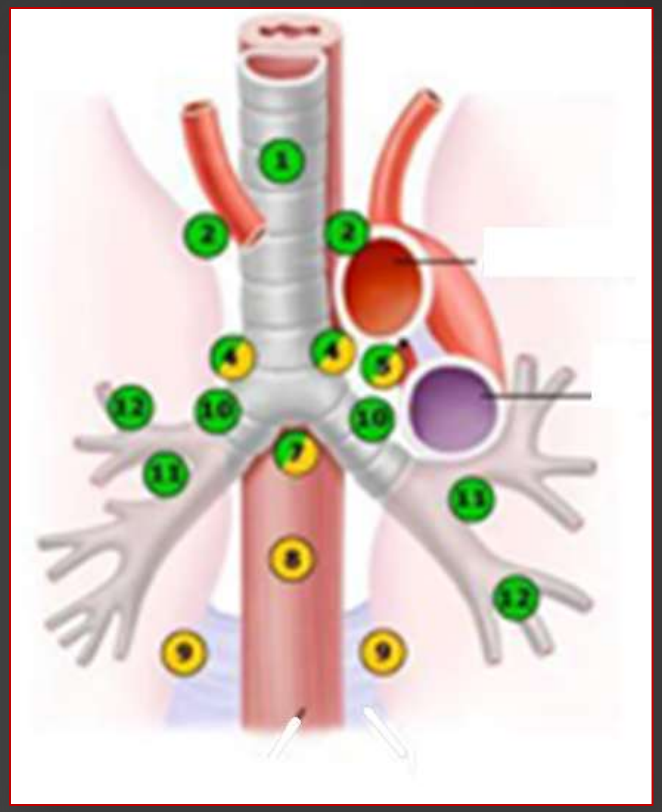

(EBUS-TBNA)

(EUS-FNA)

EBUS-TBNA)(EUS-FNA)

CONTROVERTIDO

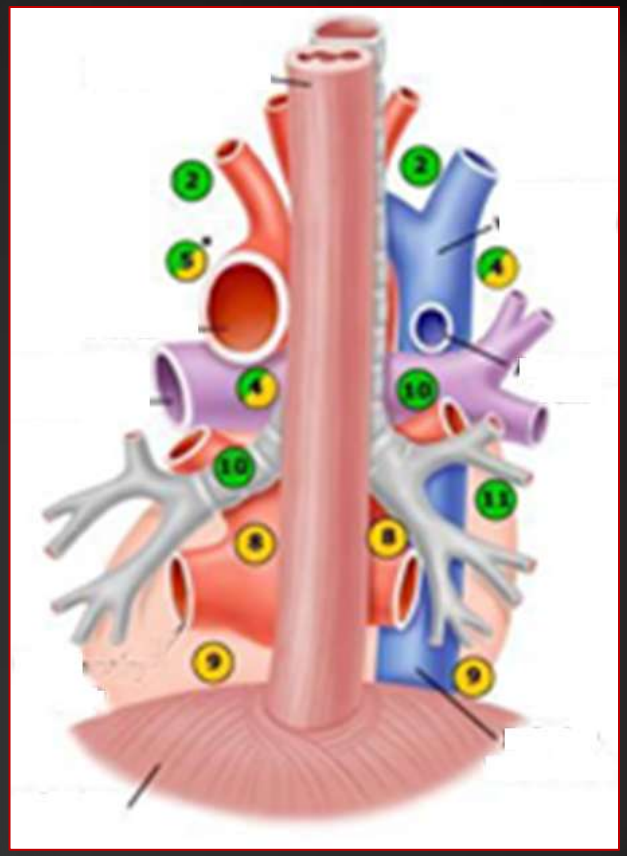

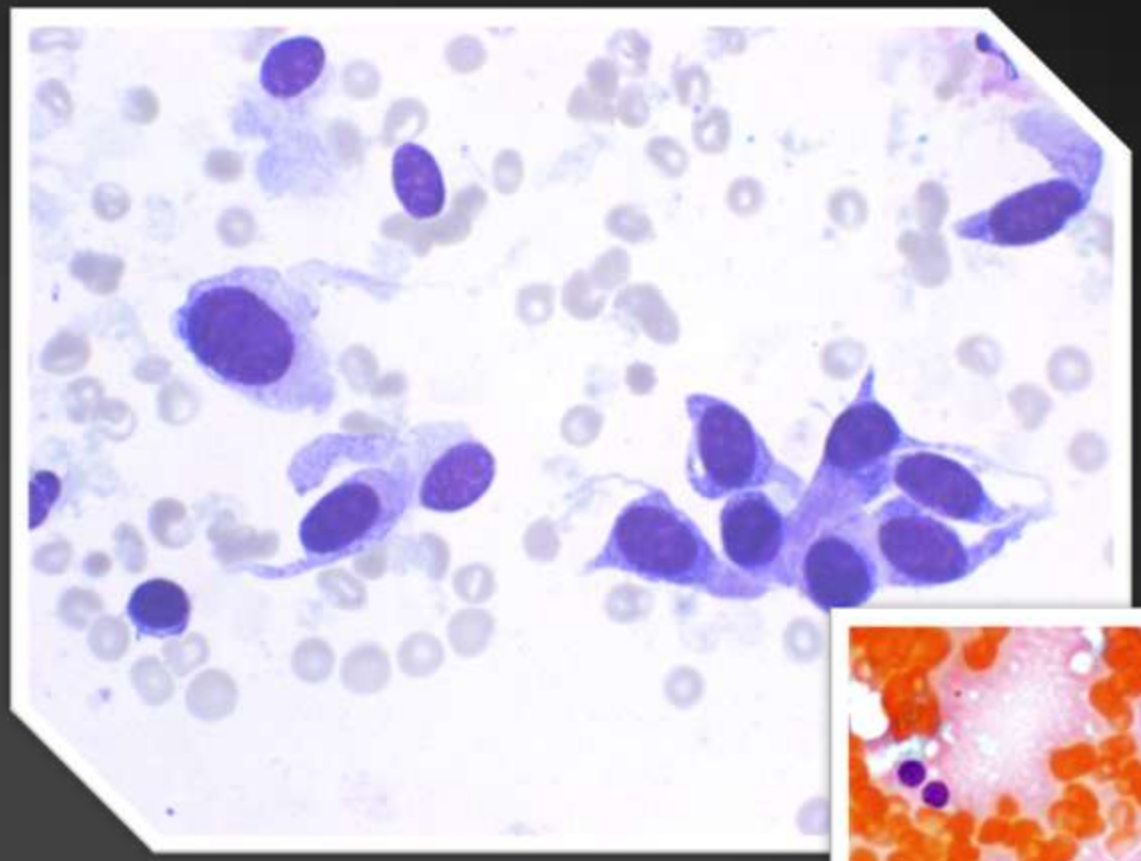

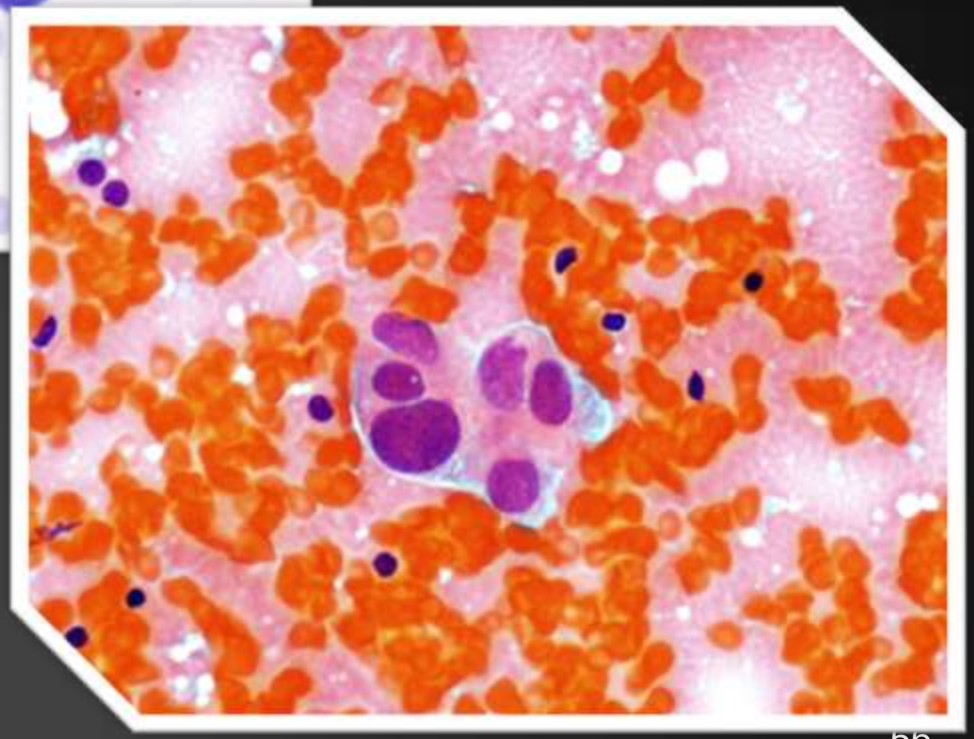

DIAGNÓTICO DIFERENCIAL. FONDO

Necrotico	*Mucinoso*	*Tigroide*	*Linfoide*
Granulomas	Contaminación	Disgrminoma /Seminoma	Adecuado Linfocitos
Tumores de alto grado	Contaminacion (Linfocitos)	Tumores con glucógeno C. Epidermoide S. Ewing's T. Células claras Otros	Linfoma
	Adenocarcinoma Mucinoso		Semejando tumores de células pequeñas azules
	Tumor quístico Mucinoso Tumor maligno con contaminación mucinosa		

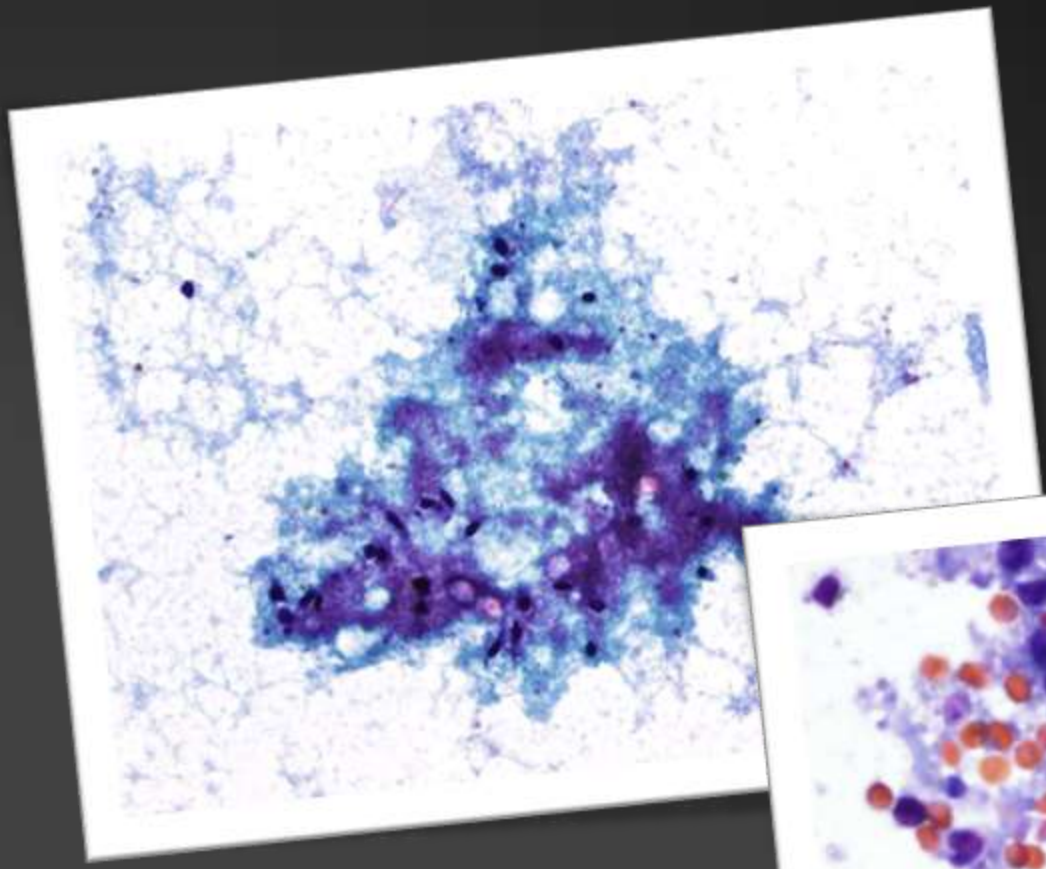

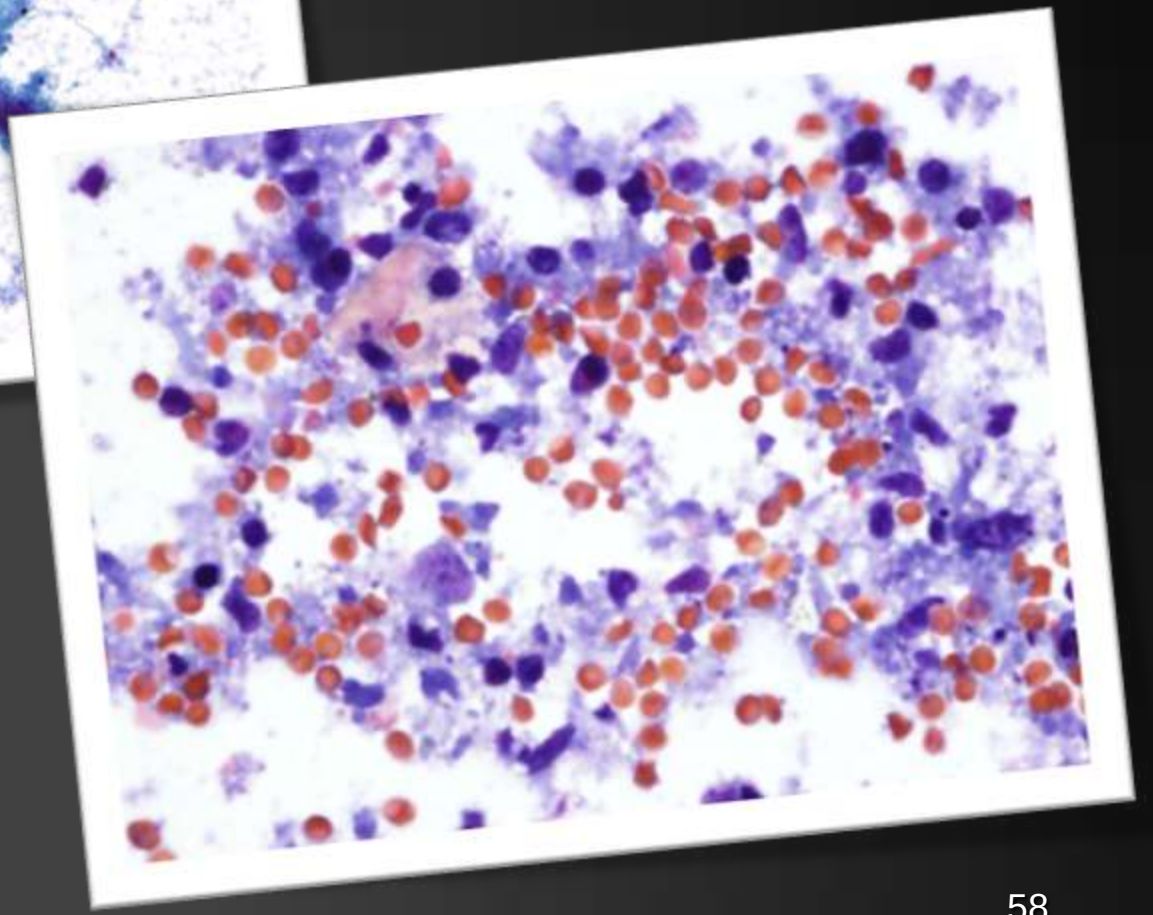

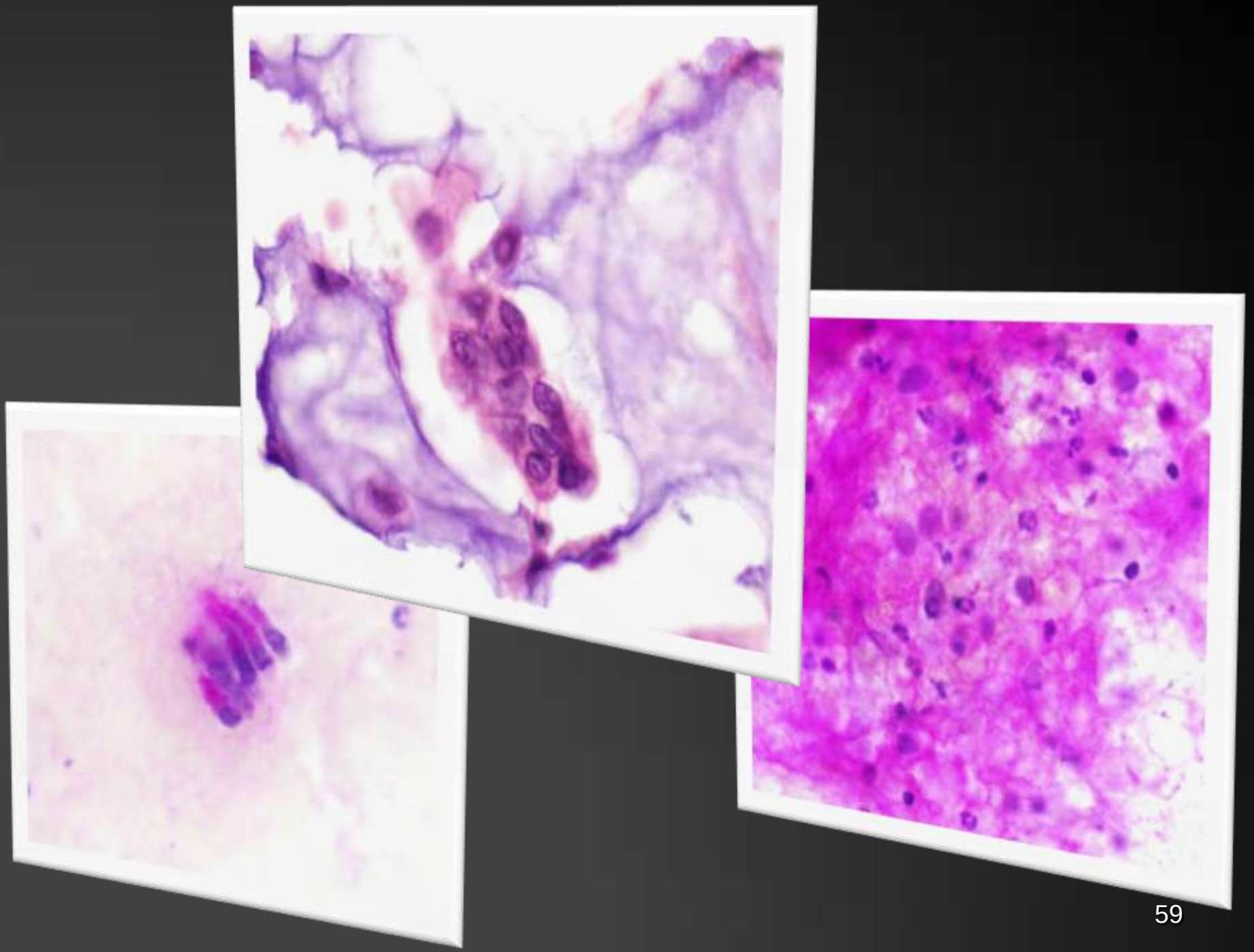

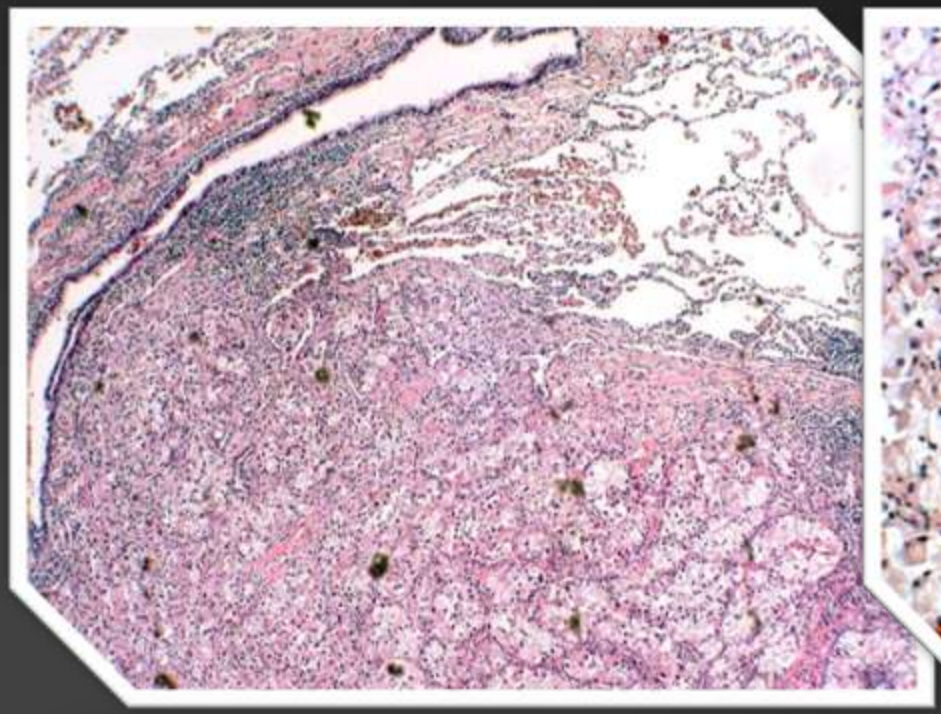

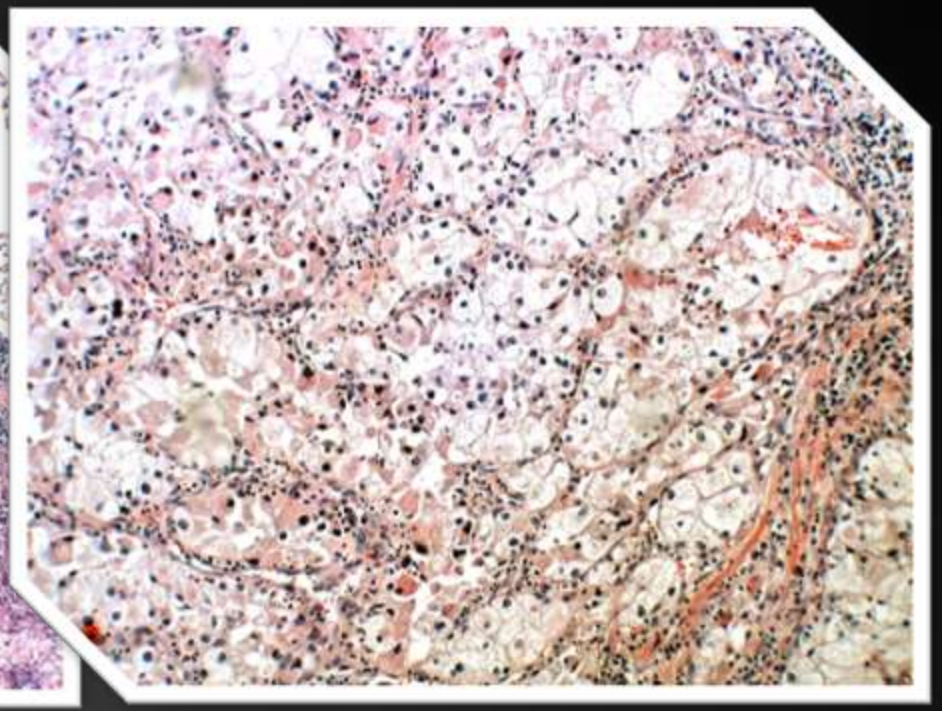

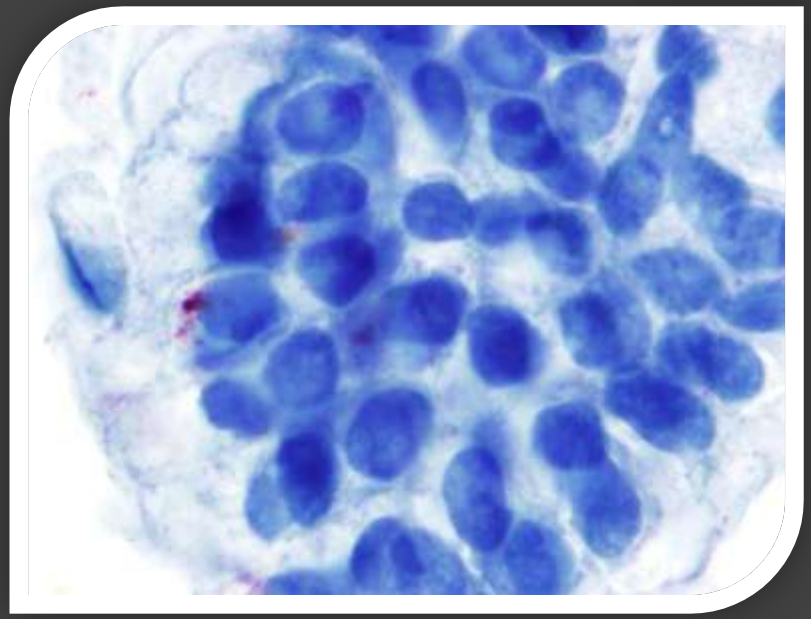

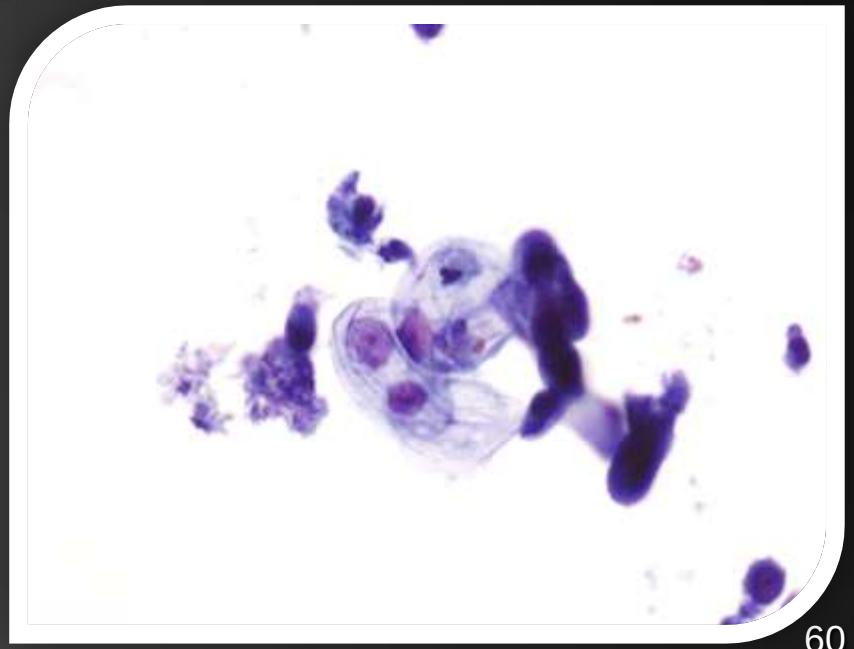

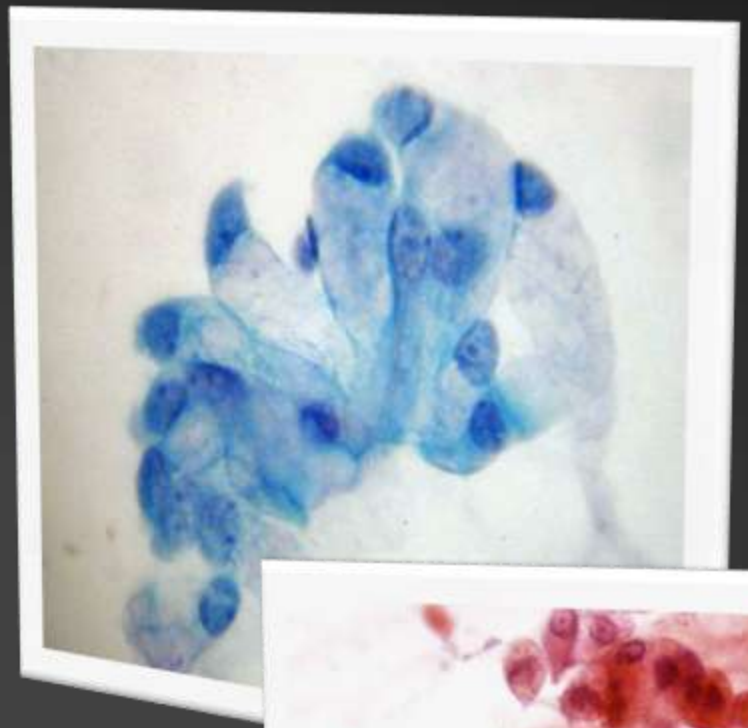

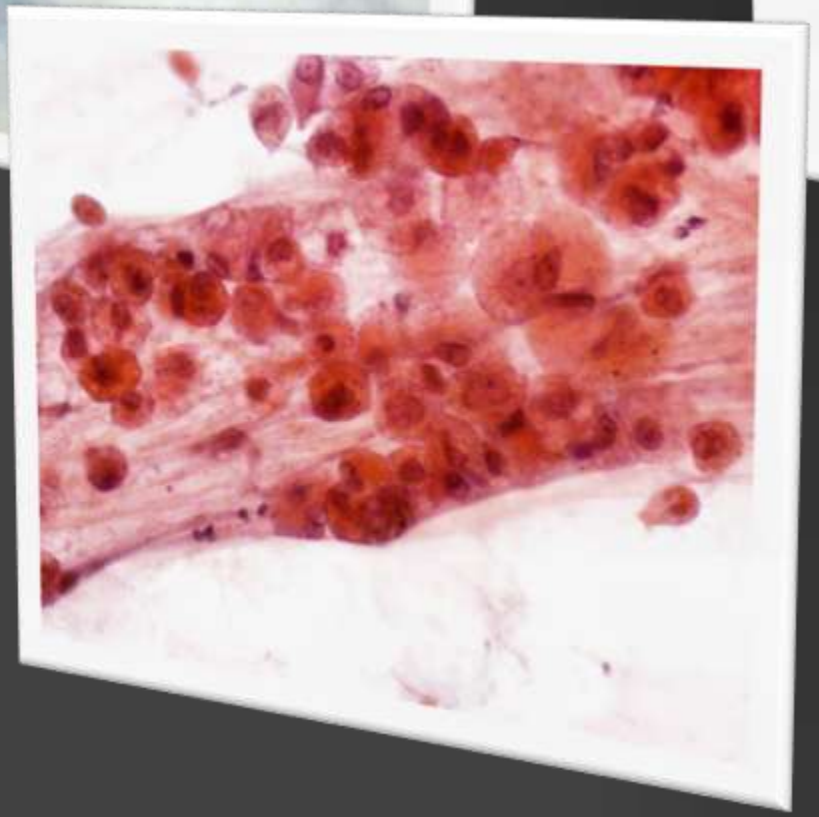

CÉLULAS ANILLO DE SELLO

Plasmocitomas

Melanomas

Mesoteliomas

Seminomas

Schwanomas

T. EWING

Mujer 22 años
Nódulo Pulmonar
Adenopatías

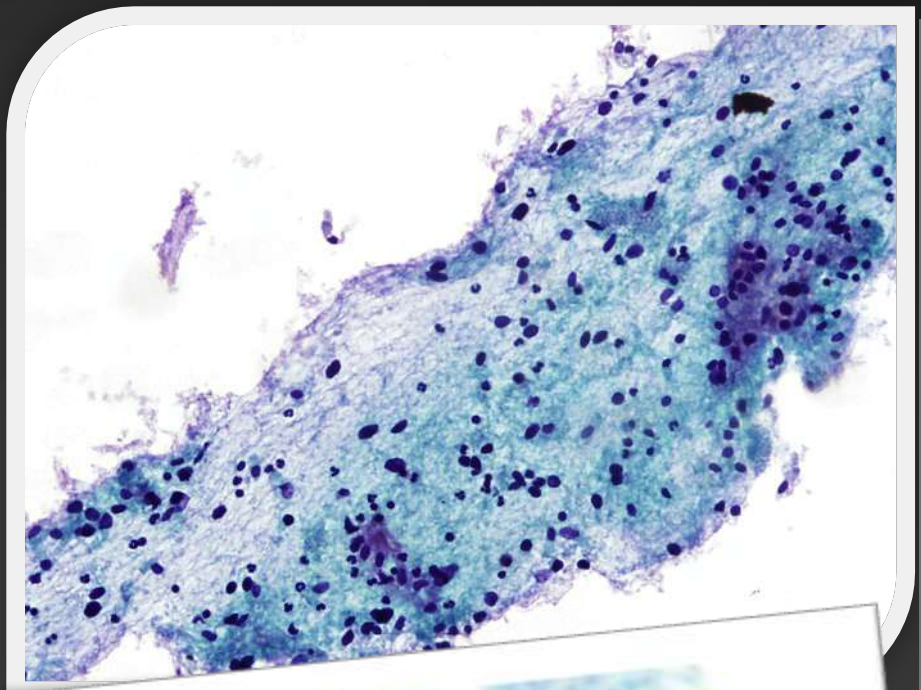

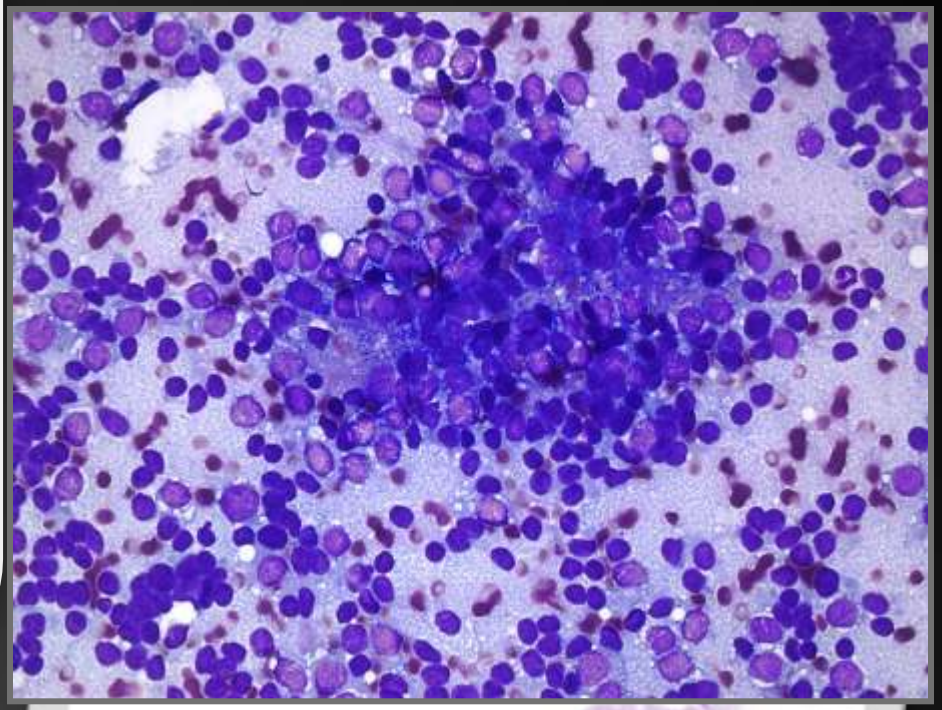

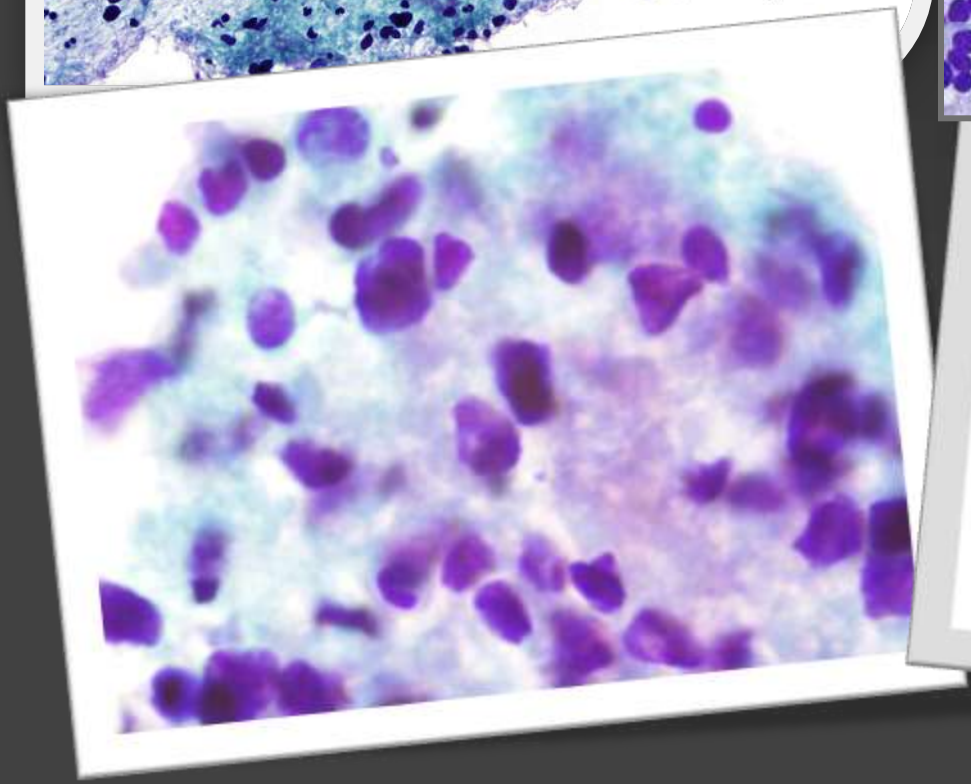

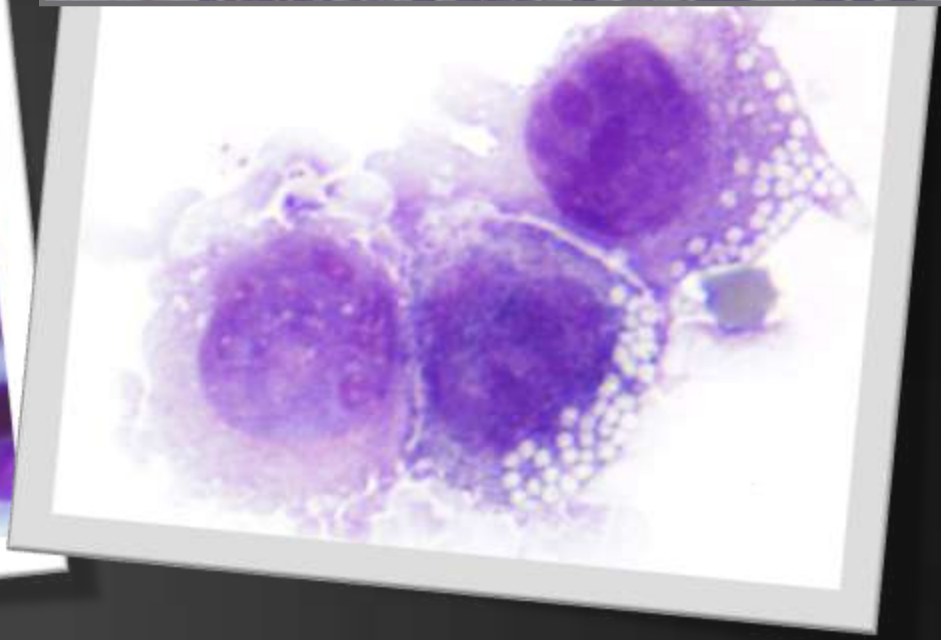

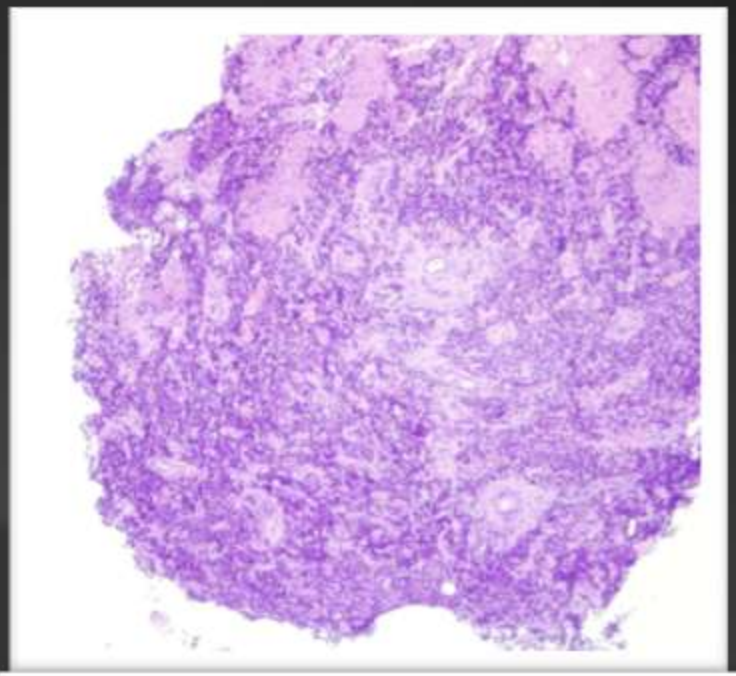

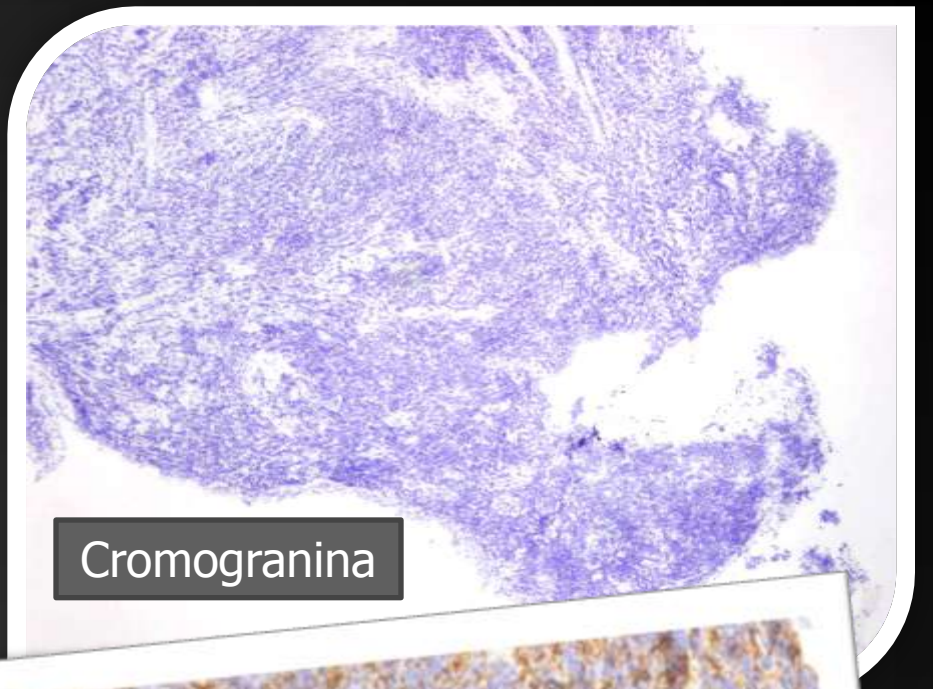
Cromogranina

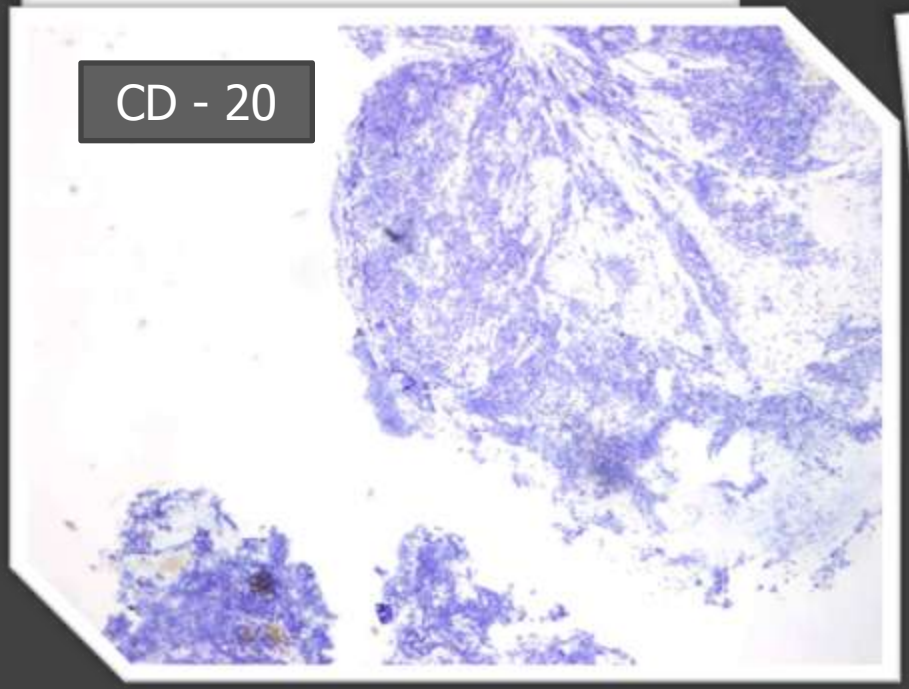
CD - 20

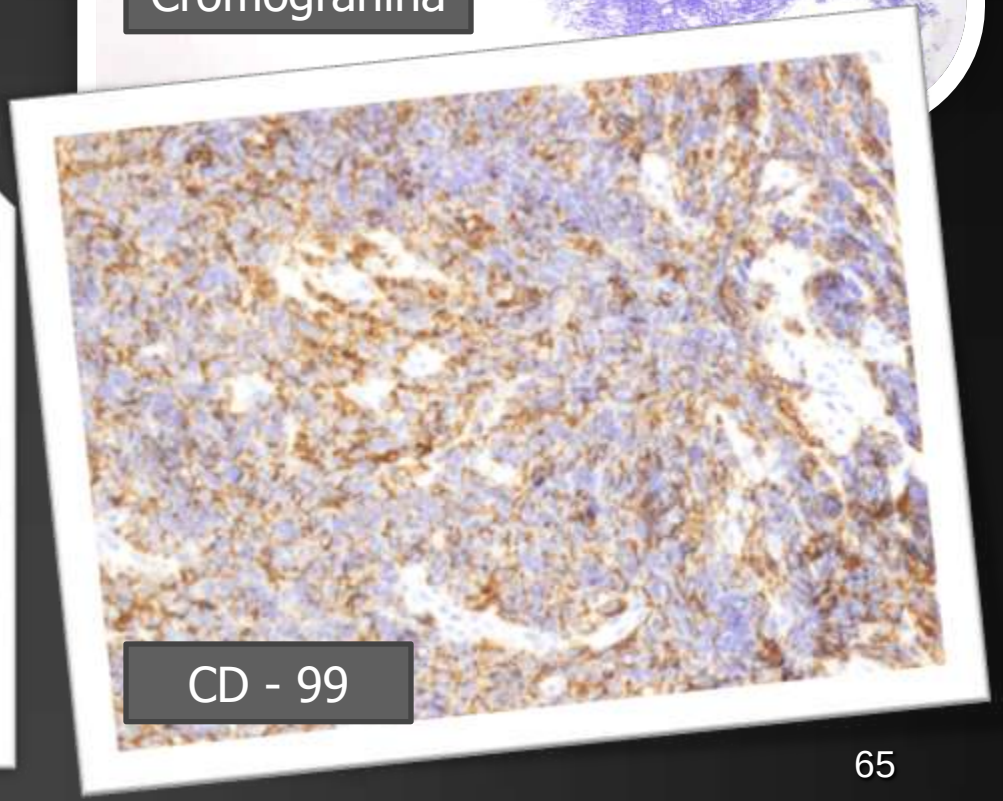
CD - 99

FONDO TIGROIDE

Seminoma / Disgerminoma
Sarcoma de Ewing
Tumores de Células Claras
Carcinoma Epidermoide
Rabdomiosarcoma
Sarcoma Sinovial


Seminoma

INMUNOHISTOQUÍMICA

	Seminoma Disgerminoma	C. Escamoso	S. Ewing
Citoqueratina		+	
CK 5/6		+	
p63		+	
Plap	+		
C-Kit	+		
Oct ¾	+		
CD 99			+

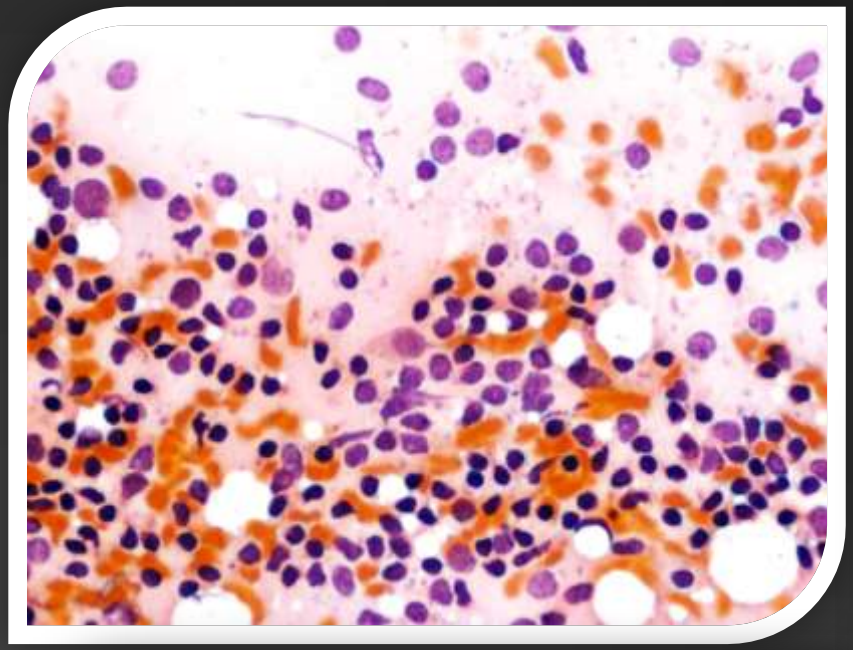

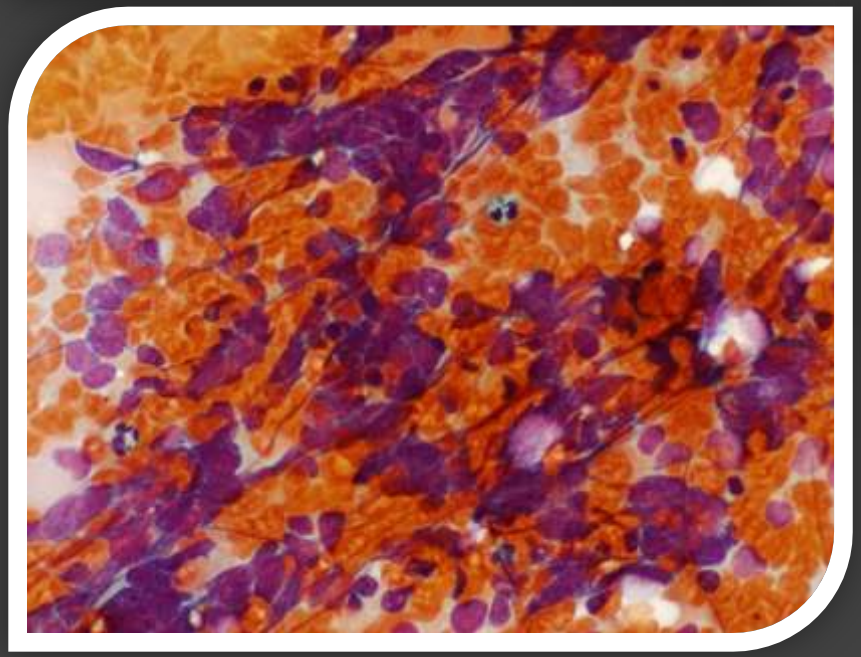

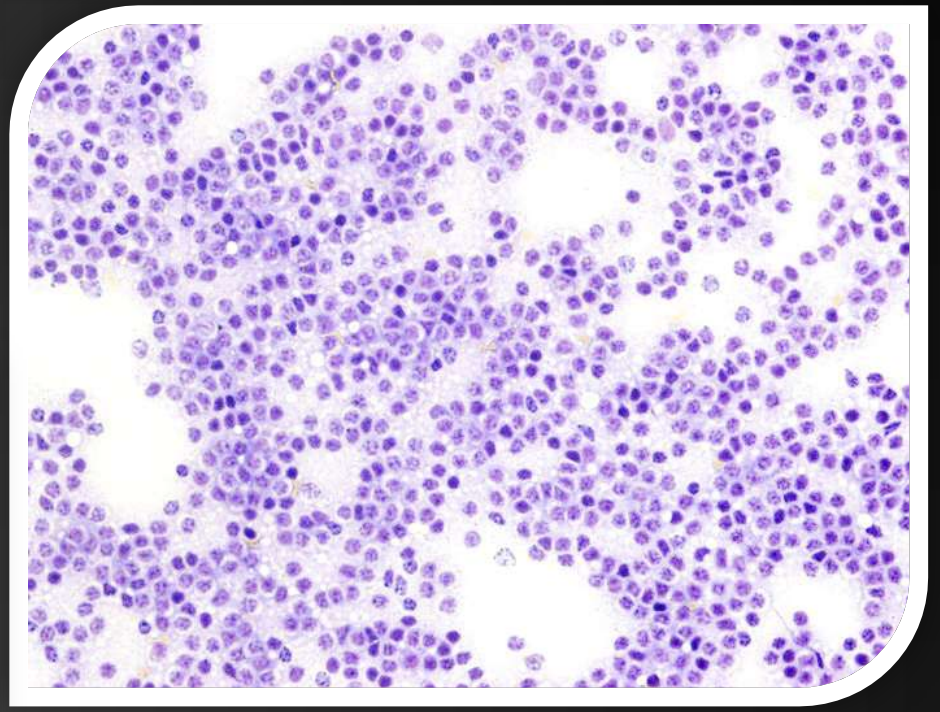

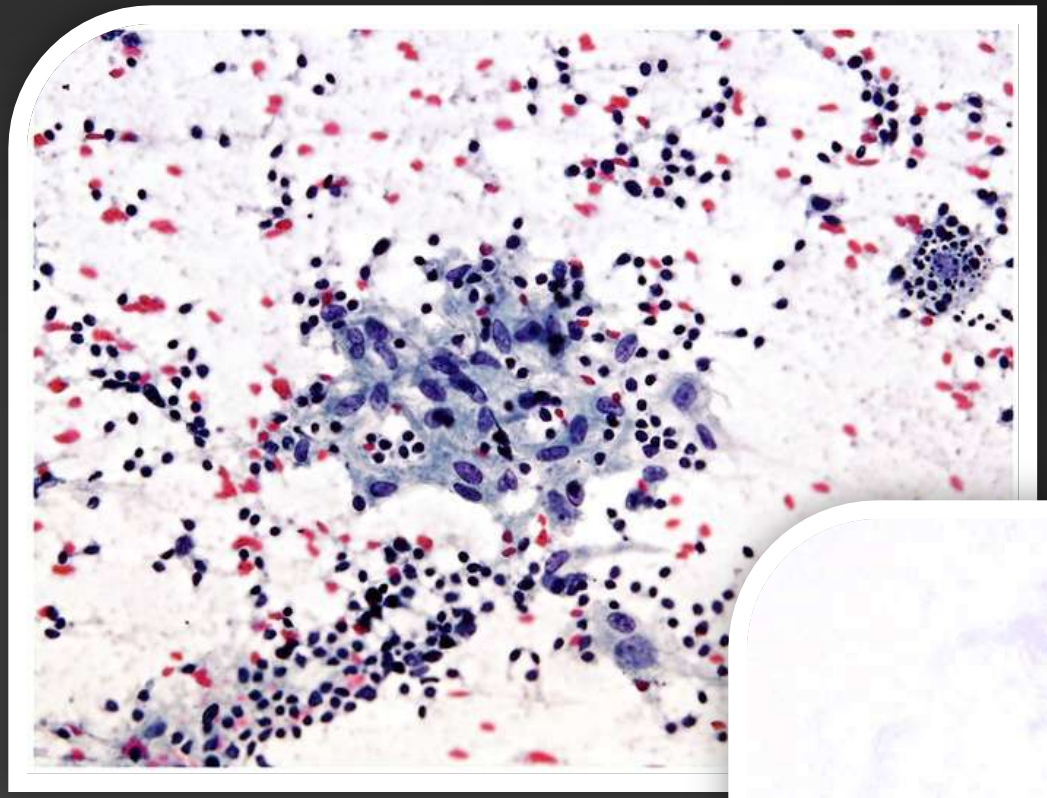

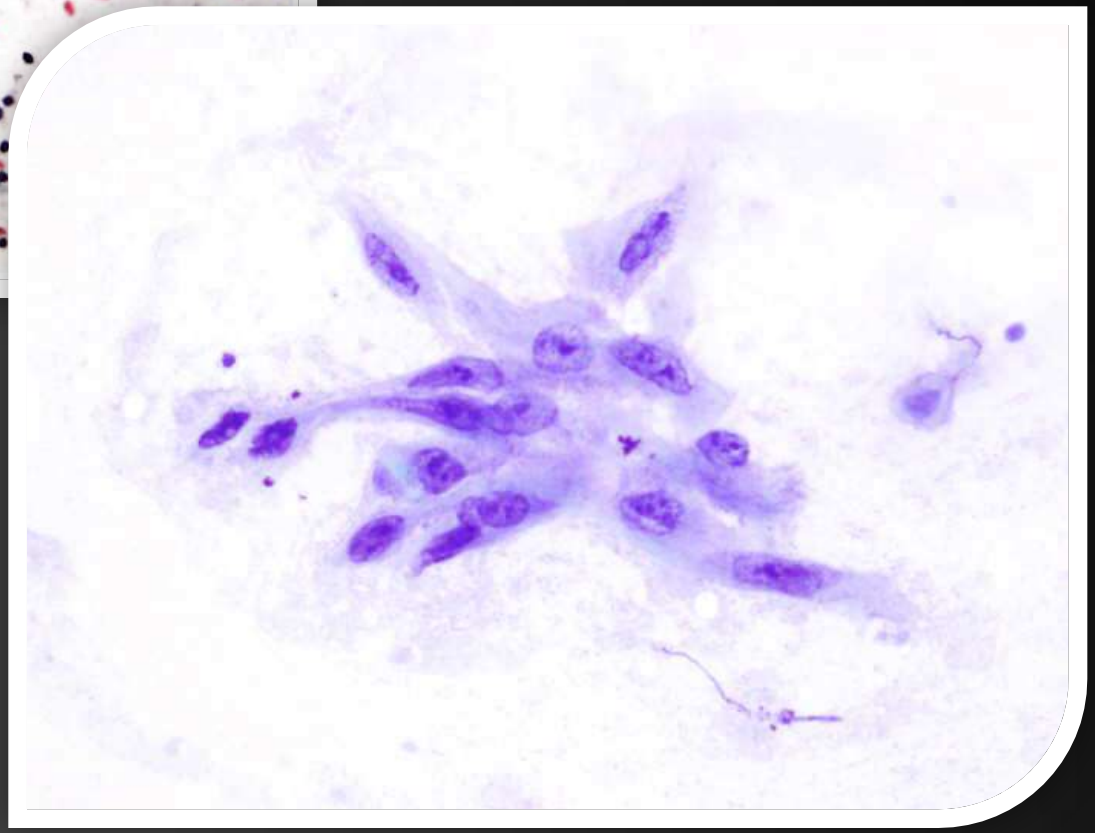

TUMORES / REACCIÓN GRANULOMATOSA

C. EPIDERMOIDE

E. HODGKIN

L. DIFUSO de C. GRANDES

C. ANAPLÁSICO de TIROIDES

C. LINFOEPITELIAL

L. ZONA MARGINAL

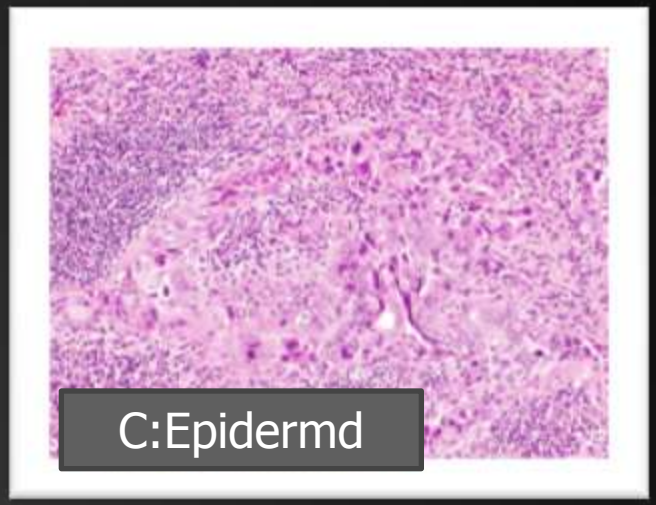

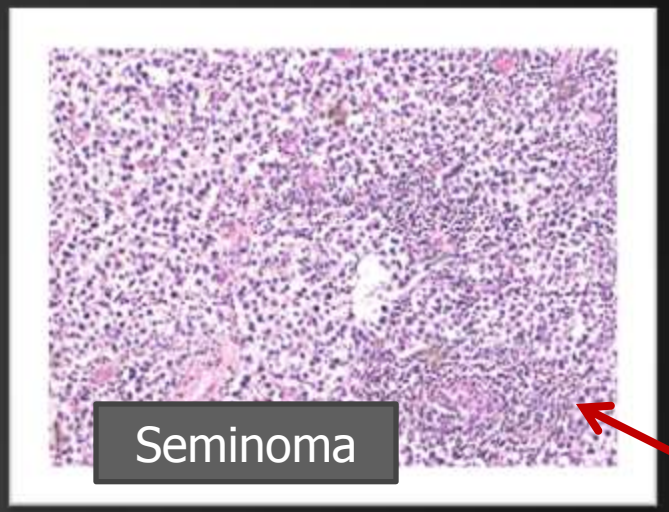

	C. ESCAMOSO	ADENOCARCINOMA
Ck 5/6	+	-
Ck 7	-	+
Ck 13	+	-
Ck 16	+	-
Ck 17	+	-
TTF-1	-	+
Napsina	-	+
Desmocolina CDSC-3	+	-
p 63	+	-

RECEPTOR FACTOR EPIDEMICO DE CRECIMIENTO

ADENOCARCINOMA 40 %

	ADENOCARCINOMA	C. ESCAMOSO
Pemetrexed	Sí	No
Bevacizumab	Sí	Hemorragias


fin